NAVAL POSTGRADUATE SCHOOL
Monterey, California

THESIS

A MATHEMATICAL MODEL OF KNEE KINEMATICS UTILIZING THE PRINCIPLE OF MINIMUM ENERGY

by

Patricia F. Warren

June 1998

Thesis Advisor: Young W. Kwon
Co-Advisor: William B. Maier II

Approved for public release; distribution is unlimited.

REPORT DOCUMENTATION PAGE

Form Approved
OMB No. 0704-0188

1. AGENCY USE ONLY *(Leave blank)*	2. REPORT DATE	3. REPORT TYPE AND DATES COVERED
	June 1998	Master's Thesis

4. TITLE AND SUBTITLE
A MATHEMATICAL MODEL OF KNEE KINEMATICS UTILIZING THE PRINCIPLE OF MINIMUM ENERGY

5. FUNDING NUMBERS

6. AUTHOR(S)
Patricia F. Warren

7. PERFORMING ORGANIZATION NAME(S) AND ADDRESS(ES)
Naval Postgraduate School
Monterey, CA 93943-5000

8. PERFORMING ORGANIZATION REPORT NUMBER

9. SPONSORING / MONITORING AGENCY NAME(S) AND ADDRESS(ES)

10. SPONSORING / MONITORING AGENCY REPORT NUMBER

11. SUPPLEMENTARY NOTES
The views expressed in this thesis are those of the author and do not reflect the official policy or position of the Department of Defense or the U.S. Government.

12a. DISTRIBUTION / AVAILABILITY STATEMENT
Approved for public release; distribution is unlimited.

12b. DISTRIBUTION CODE

13. ABSTRACT *(maximum 200 words)*

This thesis seeks to determine if the path of motion of the knee in passive flexion results from the minimization of potential energy in the joint ligaments. To investigate this hypothesis, a simulation modeling both collateral and cruciate ligaments was developed, with each cruciate ligament represented as two separate fibers. The model computed almost 8000 possible orientations of the femur during flexion through 120°, with the surfaces of the femur and tibia serving as a constraint to motion. Each orientation of the femur inherently provided the position of the individual ligament attachment points, from which the extension or contraction and the potential energy of the ligament were derived. The energy of the entire six-ligament system resulted from the summation of the potential energy of individual ligaments. For each 10° of flexion, the femur position that produced the minimum energy of this six-ligament system was identified. Finally, the motion of the femur as it followed these positions was evaluated: it did not mirror known joint motion. There are several areas where further refinement of the simulation can be made before a complete evaluation of the hypothesis can be made.

14. SUBJECT TERMS	15. NUMBER OF PAGES
energy minimization; knee; flexion; ligament	77
	16. PRICE CODE

17. SECURITY CLASSIFICATION OF REPORT	18. SECURITY CLASSIFICATION OF THIS PAGE	19. SECURITY CLASSIFICATION OF ABSTRACT	20. LIMITATION OF ABSTRACT
Unclassified	Unclassified	Unclassified	UL

NSN 7540-01-280-5500 Standard Form 298 (Rev. 2-89)

Approved for public release; distribution is unlimited

A MATHEMATICAL MODEL OF KNEE KINMATICS UTILIZING THE PRINCIPLE OF MINIMUM ENERGY

Patricia F. Warren
Lieutenant Colonel, United States Marine Corps
B.S., The University of California, Berkeley, 1980

Submitted in partial fulfillment of the
requirements for the degree of

MASTER OF SCIENCE IN APPLIED PHYSICS

from the

NAVAL POSTGRADUATE SCHOOL
June 1998

Author: 
Patricia F. Warren

Approved by: 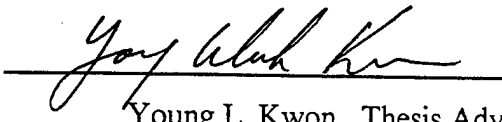
Young L. Kwon, Thesis Advisor

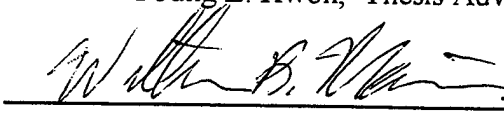
William B. Maier, Co-Advisor

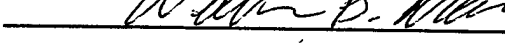
William B. Maier, Chairman
Department of Physics

ABSTRACT

This thesis seeks to determine if the path of motion of the knee in passive flexion results from the minimization of potential energy in the joint ligaments. To investigate this hypothesis, a simulation modeling both collateral and cruciate ligaments was developed, with each cruciate ligament represented as two separate fibers. The model computed almost 8000 possible orientations of the femur during flexion through 120°, with the surfaces of the femur and tibia serving as a constraint to motion. Each orientation of the femur inherently provided the position of the individual ligament attachment points, from which the extension or contraction and the potential energy of the ligament were derived. The energy of the entire six-ligament system resulted from the summation of the potential energy of individual ligaments. For each 10° of flexion, the femur position that produced the minimum energy of this six-ligament system was identified. Finally, the motion of the femur as it followed these positions was evaluated: it did not mirror known joint motion. There are several areas where further refinement of the simulation can be made before a complete evaluation of the hypothesis can be made.

TABLE OF CONTENTS

I. INTRODUCTION 1

A. PREVIOUS WORK 1

B. IMPORTANCE OF RESEARCH 3

C. OBJECTIVE OF RESEARCH 4

D. MILITARY RELEVANCE 4

II. METHODOLOGY 7

A. PHYSIOLOGY OF THE KNEE 7
1. Surface Definition 7
2. Ligament Attachment Points 9

B. SIMULATION OF KNEE KINEMATICS 11
1. Coordinate Systems 11
2. Kinematic Definitions 12
a. Background 12
b. Flexion 12
c. Internal and External Rotation 13
d. Varus-Valgus Rotation 15
e. Translation 15
3. Simulation Algorithm 16
a. Distance Algorithm 16
b. Achieving Stability: Contact in both Condyles 17

C. COMPUTATION OF POTENTIAL ENERGY 19

D. PRETENSIONING 21

E. ACL AND PCL DEFICIENT MODELS 22

III. RESULTS 23

A. POTENTIAL ENERGY CURVES 23
1. Without Pretensioning 24
2. Pretensioned Ligaments 26
3. ACL Deficient 29
4. PCL Deficient 31

B. FEMUR ORIENTATION THROUGHOUT FLEXION 33
1. Proximal-Distal and Anterior-Posterior Translation 33

a. Previous Research 33
b. Simulation Results (No Pretensioning) 33
c. Simulation Results (With Pretensioning) 38
d. Simulation Results for ACL Deficient Knee 40
e. Simulation Results for PCL Deficient Knee 43
2. Internal-External and Varus-Valgus Rotation 45
a. Previous Research 45
b. Simulation Results (No Pretensioning) 47
c. Simulation Results (With Pretensioning) 48
d. Simulation Results for ACL Deficient Knee 49
e. Simulation Results for PCL Deficient Knee 50

C. LIGAMENT LENGTH 51

1. Anterior Cruciate Ligament 53
a. Previous Research 53
b. Simulation Results 54
2. Posterior Cruciate Ligament 55
a. Previous Research 55
b. Simulation Results 56
3. Collateral Ligaments 57

IV. CONCLUSIONS 59

GLOSSARY OF MEDICAL TERMS 61

LIST OF REFERENCES 63

BIBLIOGRAPHY 65

INITIAL DISTRIBUTION LIST 67

I. INTRODUCTION

The motion of the knee is a result of the muscle forces, the articular surfaces, and the ligament structures that comprise the joint. When injured, the surgeon strives to replicate the motion of the healthy knee in order to restore normal functioning of the joint. There have been extensive studies to define that motion and thus provide critical information to the surgeon.

A. PREVIOUS WORK

Crowninshield, Pope and Johnson developed a mathematical model of the knee, that utilized thirteen ligaments whose attachment sites were determined as an average of seven cadavers specimens [Ref. 1:p. 397]. For every 10° of neutral flexion, this simulation first rotated the femur in internal-external rotation, then in varus-valgus rotation before translating it first in the proximal-distal direction, and then in the anterior-posterior direction [Ref. 1:p. 398]. The study does not state the range of motion that was evaluated for each of these degrees of freedom nor does it state how the articular surfaces were modeled or if they played a role in determining the allowable range of motion of the joint. The cross-sectional area of each ligament was utilized in determining the force required to stretch a ligament [Ref. 1:p. 401], however, the stiffness was invariant between ligament structures [Ref. 1:p. 400].

Essinger, Leyvraz, Heegard and Robertson developed a simulation of a mechanical jig that is often used to test flexion of cadaver knees. Flexing the knees through 120° by simulating muscle forces, the model finds the position of the femur that minimizes the potential energy of the system. The system evaluated included ligaments that were modeled as seven springs with a non-linear elastic representation of the force-

elongation function for each ligament. The tibial surface was also included in the model. It was simulated as a deformable entity, similar to a sheet of vertical springs, and was allowed to compress without bound in order to accommodate femoral displacement into the tibia. Also incorporated into the model were the potential energy of the patella ligament and the energy resulting from the displacement of body weight. Anatomical data from 10 cadaver knees were input into the simulation and the results, to include the motion pattern and ligament length, compared favorably against other studies. Again, the range of allowable motion of the femur was not specified in their paper; nor was there any delineation of permissible tibial deformation. Thus, the role of the femoral and tibial surfaces in providing a constraint to motion was not evaluated. [Ref. 2]

In the mathematical model developed by Wismans, Veldpaus and Janssen, the motion and forces between the tibia and femur were evaluated. Seven ligaments were incorporated into the simulation and equations of force and moment equilibrium, consisting of ligament and capsule forces and external forces of muscles, inertia, and patella, were solved for femoral positional information. This model provided a description of the motion path of the femur as it flexed through 100°. Results for several ligaments appeared to be representative of experimental results. However, the cruciate ligaments were modeled by only a single fiber thus it is not possible to fully evaluate the accuracy of the model. Additionally, as the study measured 100-200 points on each bone and developed best fit polynomials to describe each articular surface, the accuracy of the bones as a constraint to motion is questionable. [Ref. 3]

B. IMPORTANCE OF RESEARCH

Even if joint motion were to be accurately and precisely defined, there is a uniqueness to each individual's knee, owing to age, sex, levels of motion, etc., [Ref. 4:p. 115]. These differences are manifest in variations in ligament length, in the position of the ligament insertion sites and in the articular surfaces of the femur and tibia [Ref. 5:p. 148]. Thus, when ligament rupture occurs, the surgeon is unable to use a "one size fits all" approach to ligament reconstruction; he must know the individuality of the operated knee in order to restore normal function [Ref. 5:p. 148].

In particular, in replicating the normal function of an injured knee, it is of paramount importance that the proper insertion site is chosen during surgery. A site is deemed "correct" if the neutral fiber of the replacement tissue remains isometric during flexion, thereby preventing any excessive tension on the graft, to guard against rupture [Ref. 4:p 187]. The site must also prohibit undue laxity or else it will be of little use in providing guidance to the joint and will result in subsequent damage to other tissues [Ref. 4:p. 188]. It is reported by O'Connor, et. al., that it is relatively easy to identify and insert the cruciate ligaments onto the tibial surface [Ref. 4:p. 188]. However, due to the anatomy of the femur, it is much more challenging to locate the optimum cruciate insertion points on this surface; unfortunately,

> ...the percentage length change in the replacement over the flexion range is proportionately greater for malpositioning the femoral site than for malpositioning the tibial site. As a result the technically more difficult site to position is also the more critical in achieving isometric graft length [Ref. 4:p. 188].

In fact, it is not uncommon for a cruciate ligament to be emplaced too far forward, resulting in the requirement for excessive muscle forces to be generated during flexion

[Ref. 5:p. 20]. Thus, even though research on the defining the envelope of knee motion of the knee is proceeding, it is essential that for an individual to be returned to a fully functioning capability, their particular idiopathies be incorporated into the surgeon's approach to reconstruction.

C. OBJECTIVE OF RESEARCH

The objective of this thesis was to identify if the motion of the knee was based upon the principle of energy minimization, i.e., if, during passive flexion, the knee follows a path ascribed by the least energy stored within a six ligament system. The system addressed is comprised of the lateral collateral, medial collateral, and the anterior and posterior fibers of both the anterior cruciate and posterior cruciate ligaments. Unlike the aforementioned studies, this simulation incorporates the constraint imposed by the actual, articular surfaces that are assumed to be rigid and to limit motion. While it is recognized that this simulation is simplistic, if the results qualitatively support the hypothesis, then a rationale for studying a complex, more representative system can be made. Optimally, the process can be reverse engineered; that is, given the surfaces of an individual's femur and tibia, and the insertion sites of the undamaged ligaments, this research could lead to determination of the optimum position for ligament reattachment sites in reparative surgery.

D. MILITARY RELEVANCE

While this research has the potential to assist all those who undergo ligament replacement surgery, it has great applicability to United States Marine Corps. Marines undergo a demanding physical training regimen to ensure that they are prepared to meet any physical challenge they may encounter; however, an unintended consequence of this

difficult physical preparation is that Marines undergo a disproportionate number of ligament surgeries in comparison with their service counterparts. Although they comprise just over 12% of active duty military [Ref. 6], Marines require over one third of DoD cruciate ligament surgeries [Ref. 7]. Any work that assists in restoring Marines to fully functioning, combat systems will greatly aid readiness.

II. METHODOLOGY

Mapping the path of minimum strain energy requires the computation of ligament length and, therefore, the identification of the ligament attachment positions, as the knee joint transverses through the range of possible motion. Because the ligaments are affixed to the skeletal system, the positions of these attachment points are inherently determined by the orientation of the femur and tibia, as the femur is rotated and translated.

A. PHYSIOLOGY OF THE KNEE

1. Surface Definition

Since the surfaces of the femur and tibia provide a constraint to the motion of knee, it was necessary to map their topography. Foam injected models, molded from an actual tibia and femur, were used as a representative joint. With the bones in full extension, marker points were made on each bone to provide reference alignment points. Each foam-molded bone was then placed in a Puma 500 3-D Coordinate Measuring Machine and the x, y and z coordinates of almost 750 points were measured on the two surfaces. However, due to the machine configuration, the femur and the tibia had to be placed at incongruous orientations in order to map their surface contours as represented by the position of the alignment reference points, 'o's on the tibia and 'x' and '+' on the femur, in Figure 1. The limitation of the machine necessitated the development of a separate computer program that aligned the aforementioned reference points and brought the computer images of the femur and tibia into contact, in the fully extended position (Figure 2).

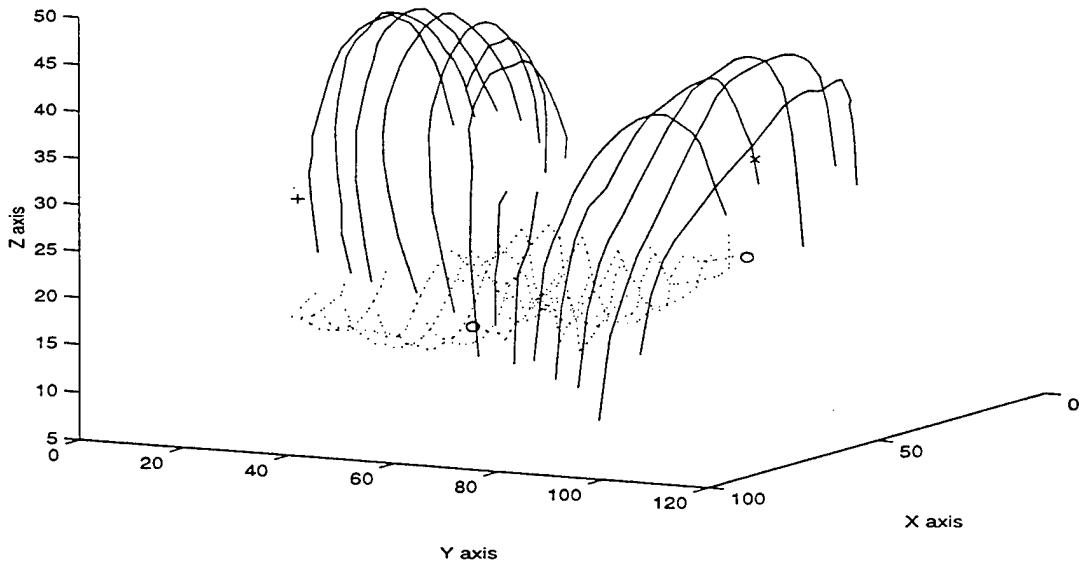

Figure 1. A Perspective View of the Orientation of the Femur and Tibia after Measurement in the Puma 500 Coordinate Measuring Machine. The femur surface is represented by solid lines; the tibia surface by dotted lines.

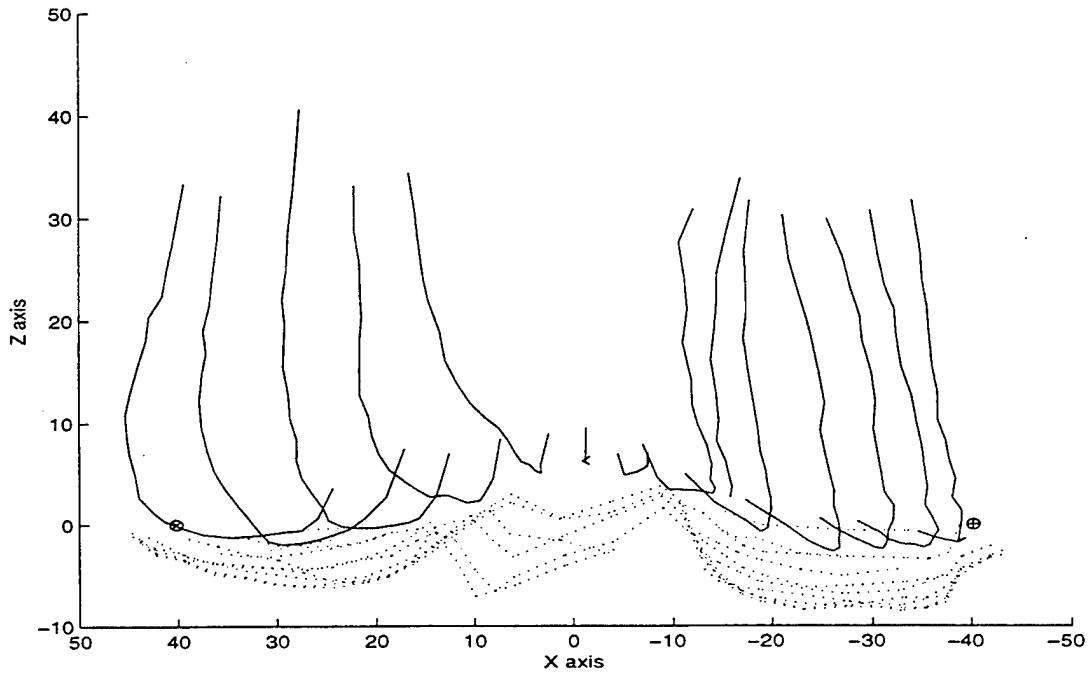

Figure 2. Anterior View of the Computer Alignment of Femur and Tibia in Full Extension. Note that the reference points are coincident. The femur surface is represented by solid lines; the tibia surface by dotted lines.

2. Ligament Attachment Points

The foam-molded model of the knee did not provide cruciate ligament attachment points on either surface. However, utilizing seven cadaver knees, Crowninshield made measurements of ligament attachment sites which showed at most 10% fluctuation between specimens [Ref. 1:p. 398]. The attachment site positions for the lateral collateral ligament (LCL), medial collateral ligament (MCL), anterior fiber of the posterior cruciate ligament (APCL), posterior fiber of the posterior cruciate ligament (PPCL), anterior fiber of the anterior cruciate ligament (AACL) and posterior fiber of the anterior cruciate ligament (APCL) were mapped to their respective locations on the computer representation of the foam surfaces. After 3-D rotation and comparison to both anatomical models and displays, they were deemed to provide an adequate representation of cruciate ligament position (Figures 3 through 5).

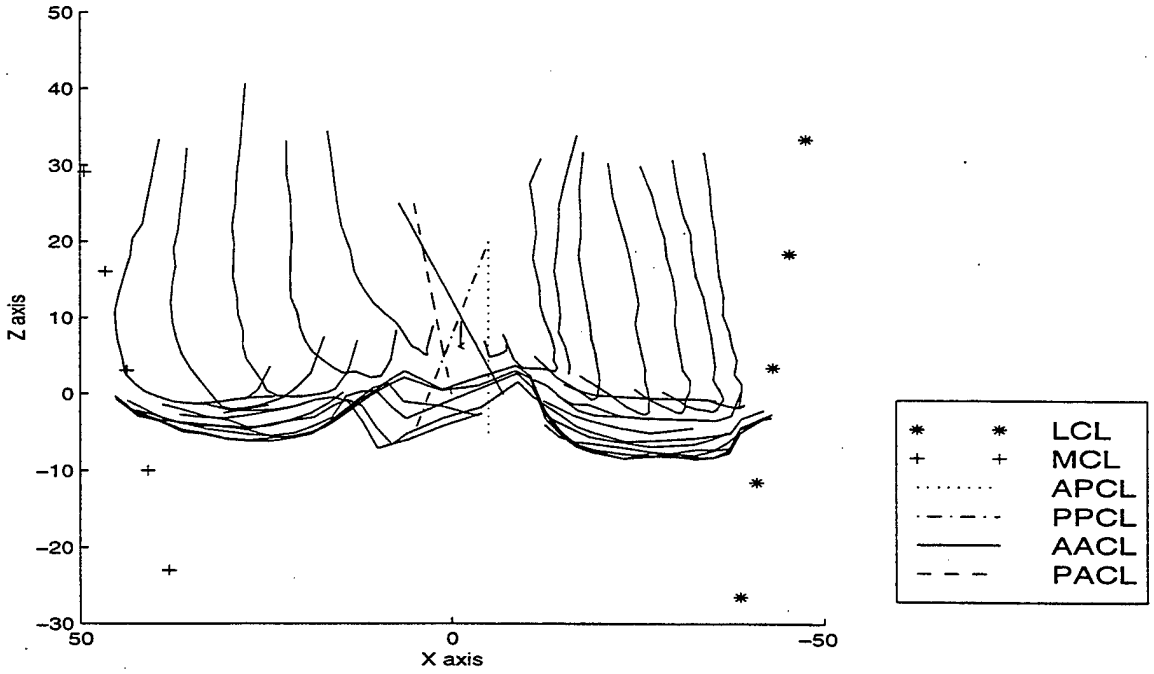

Figure 3. Anterior View of Ligaments. Femur and Tibia are depicted as solid lines in this figure.

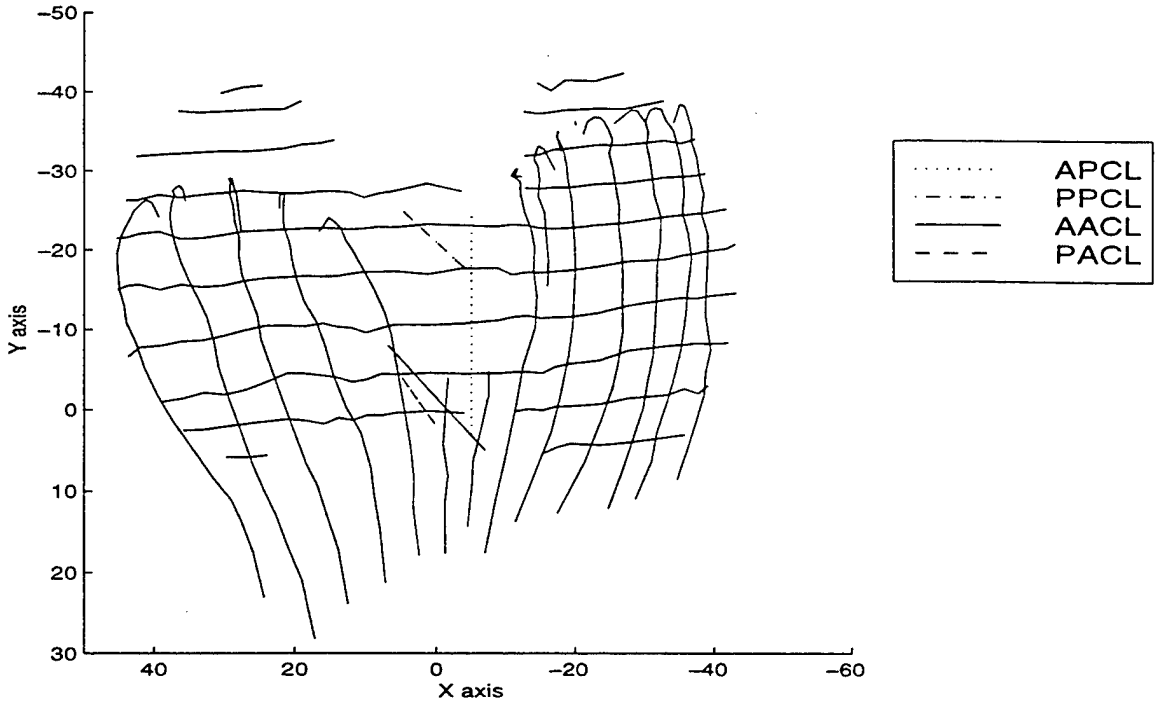

Figure 4. Proximal View of Cruciate Ligaments. The femur contours are almost vertical lines; the tibia contours are the almost horizontal lines

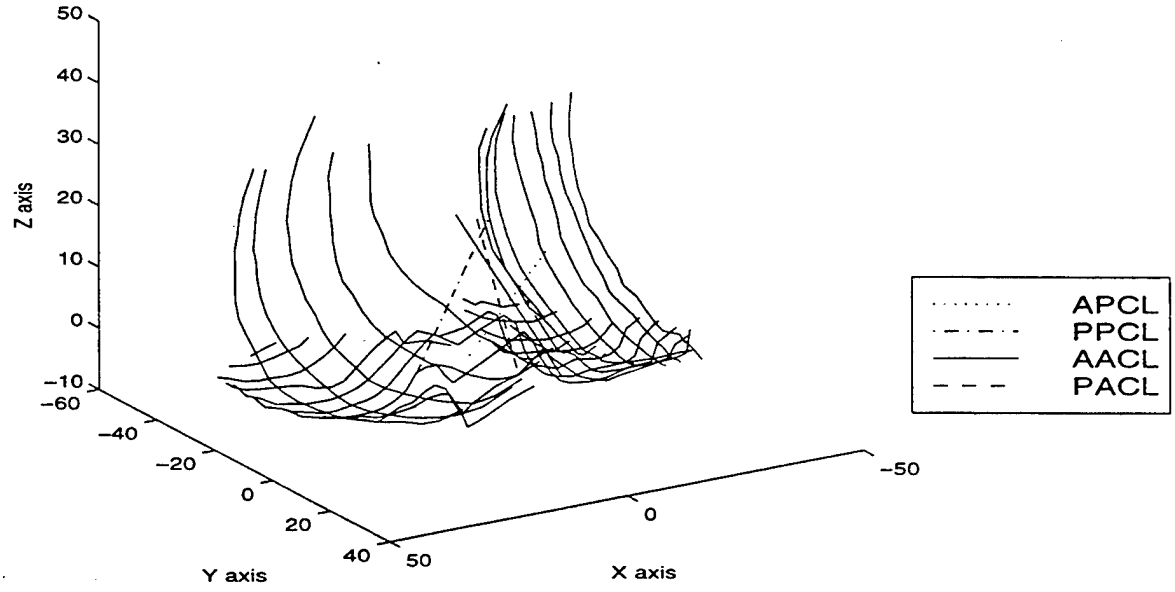

Figure 5. Perspective View of Cruciate Ligaments

B. SIMULATION OF KNEE KINEMATICS

1. Coordinate Systems

The motion of the knee can be viewed analyzed as combinations of three rotations about orthogonal axes and three translations. There were two coordinate systems utilized in this simulation. The global coordinate system was affixed to the tibia, with the origin chosen to lie midway between the aforementioned alignment points. The x-axis ran medially to laterally, through these alignment points, approximately parallel to the epicondylar axis. The y-axis is positioned posteriorly to anteriorly and the z-axis is aligned along the length of the tibial axis, distally to proximally (Figure 6). A local coordinate system, the prime coordinate system, was affixed to the femur and was co-incident with the global axis only at the position of full extension (Figure 7).

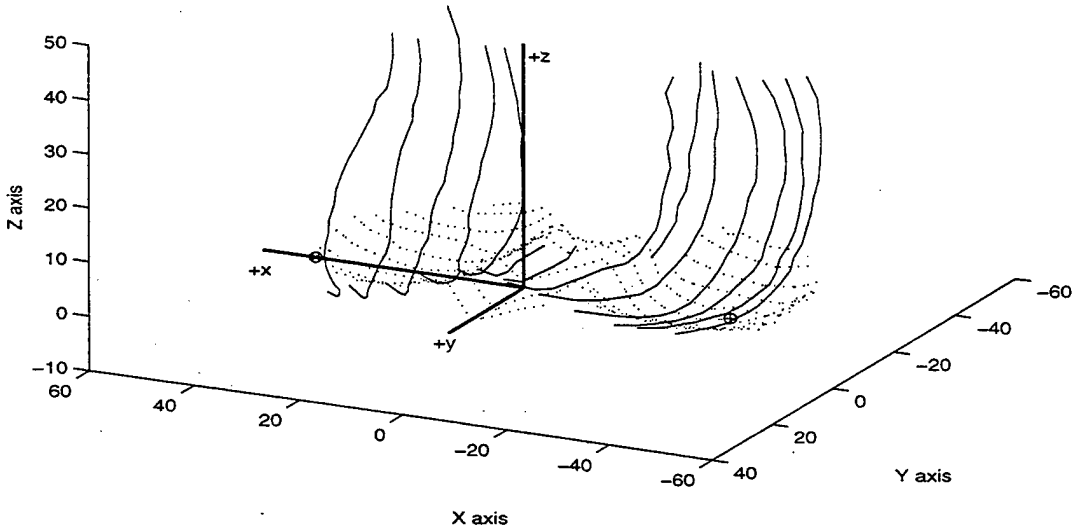

Figure 6. Global Coordinate System. The femur is represented by solid, curved lines; the tibia by dotted lines.

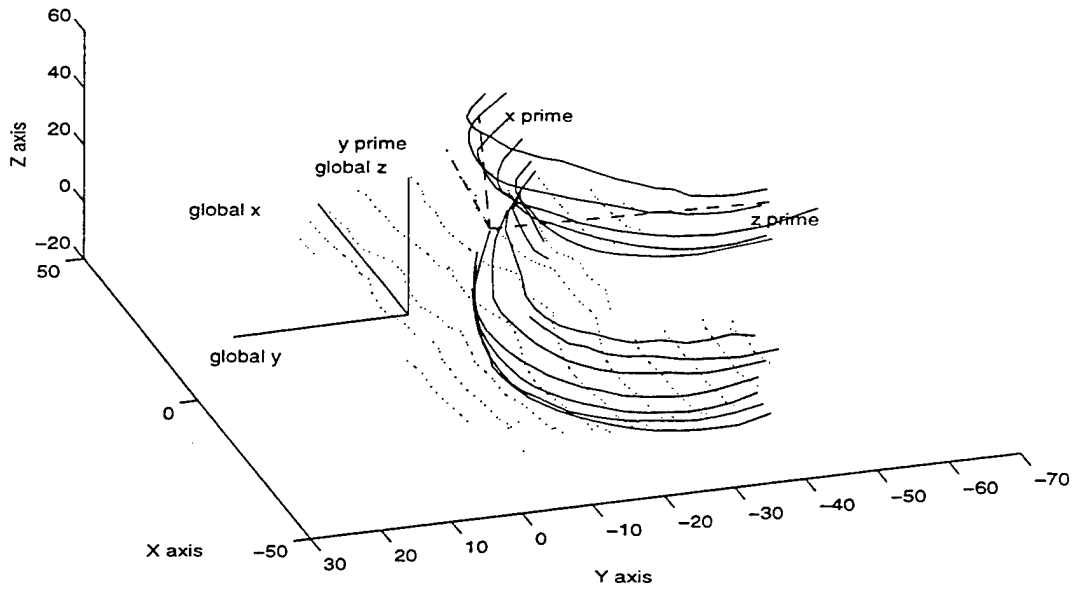

Figure 7. Depiction of Global and Local Coordinate Systems after Femur Rotation and Displacement. The contours of the femur surface are shown as curved, solid lines; the contours of the tibia surface are represented by dotted lines.

2. Kinematic Definitions

a. Background

Because of the lack of anatomical reference marks, there is neither a standard coordinate system nor definition of the descriptive terms that define knee position, i.e., flexion, internal-external and varus-valgus rotations. Because of this variability, it is necessary to define usage of these terms.

b. Flexion

In this simulation, "flexion" is used to describe the angle of rotation of the femur in the y-z plane, as measured from the global z-axis. To do this, a reference point

along the global z-axis was generated while the knee was in extension (Figure 8). This point was rotated and translated with the femur. The determination of Ψ, the rotation angle in the y-z plane, was made by constructing at the local femur origin an axis, parallel to the global z-axis, and evaluating through trigonometry the position of the constructed reference point (Figure 9).

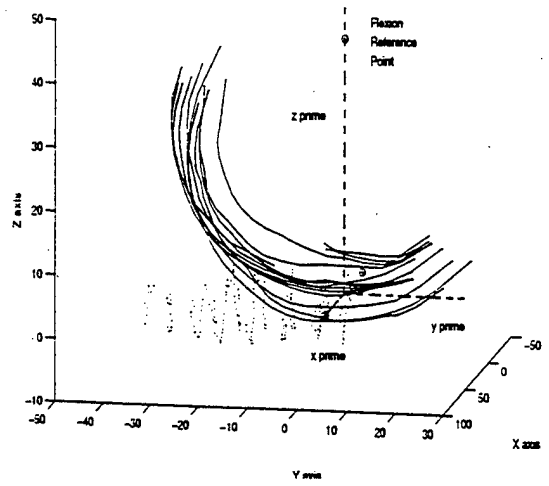

Figure 8. Lateral View of Constructed Flexion Reference Point. Femur is shown as solid line; tibia is dotted. Local axes are dashed lines.

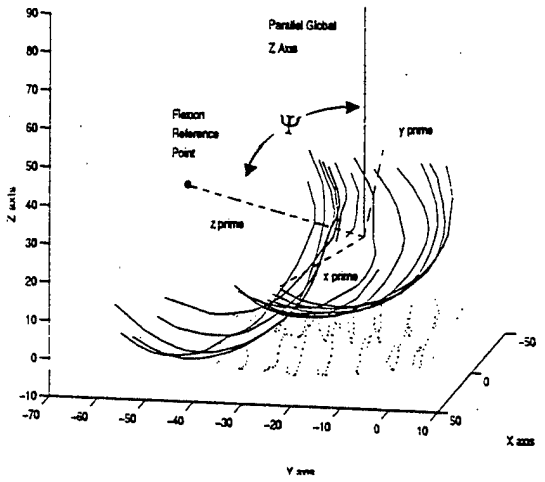

Figure 9. Position of Flexion Reference Point following Femur Rotation and Translation. Representation is as stated in previous figure.

c. Internal and External Rotation

Internal-external rotation was defined as rotation of the femur, relative to the tibia, about the global z-axis (Figures 10 and 11). A proximal perspective, with the femur flexed at 80°, displaced 12 mm posteriorly, undergoing 18° external rotation, is shown in Figure 12. Displayed also are the global and local x axes, shown as solid and

dashed lines respectively. This representation is indicative of the difficulty in defining motion of the joint.

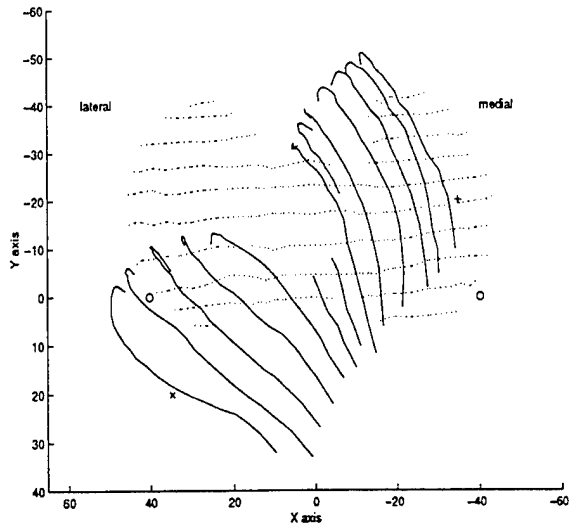

Figure 10. Proximal View of Internal Rotation of the Femur Relative to the Tibia. Femur contours are shown as solid lines; tibia contours as dotted lines. Reference alignment points are as previously described.

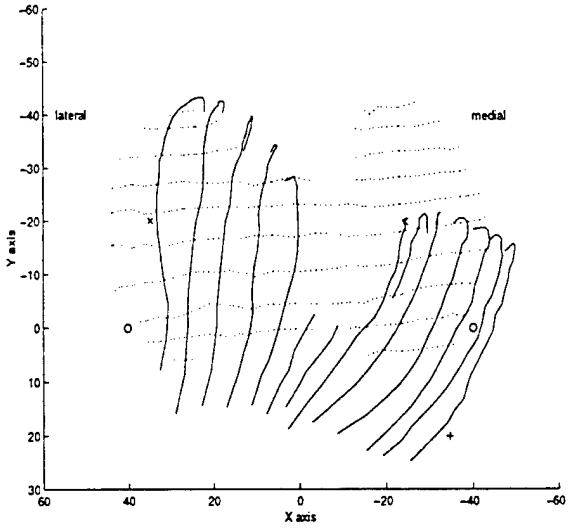

Figure 11. Proximal View of External Rotation of the Femur Relative to the Tibia. Surface representations are as stated in previous figure. Reference alignment points are as previously described.

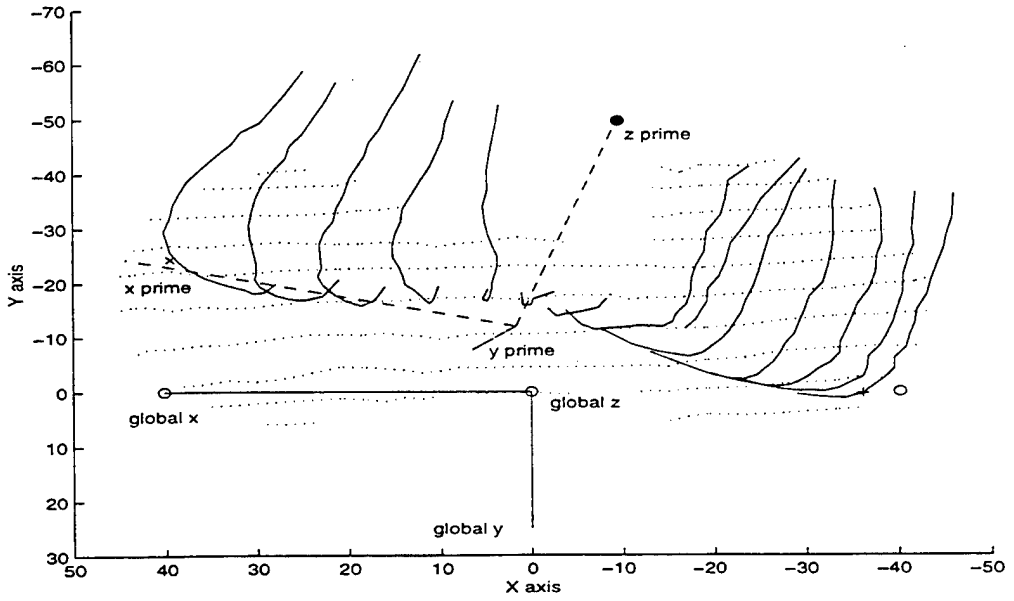

Figure 12. Proximal View of Femur: 80° Flexion, 12 mm Posterior Translation and 18° External Rotation. Surface representations and reference alignment points are as previously described. Local axis is represented by dashed lines; the global axis as solid lines.

d. Varus-Valgus Rotation

Rotation about the global y-axis defines the varus, i.e., toward the medial, or valgus, i.e., toward the lateral, rotation (Figures 13 and 14, respectively). Again, rotation was defined in terms of femur, relative to the tibia.

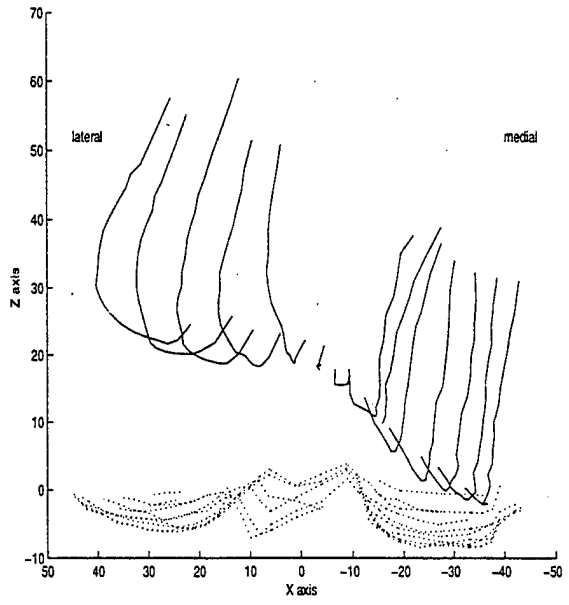

Figure 13. Anterior View of Varus Rotation of the Femur Relative to the Tibia. Femoral and Tibial surface contours are as described in previous figure.

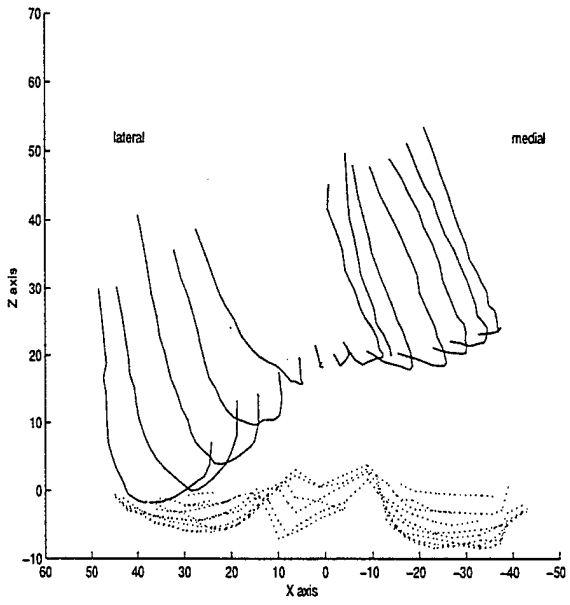

Figure 14. Anterior View of Valgus Rotation of the Femur Relative to the Tibia. Femoral and Tibial surface contours are as described in previous figure.

e. Translation

It has been demonstrated that there is significant rotation about all axes but there is only significant translation in two directions. In his experimental research, Essinger found that the medial-lateral translation was insignificant [Ref. 2:p. 1235]; it varied only about .6% of the widest lateral-medial dimension. Blankevoort's

experimental work provided further testimony to the negligibility of this translation [Ref. 8:p. 708-711]. Therefore, in developing this simulation, this degree of freedom was neglected.

3. Simulation Algorithm

For each increment of flexion, the model computed the position of the femur in 660 different configurations. For ease of computation, the program initially displaced the femur proximally by 20 mm. After rotating the femur to the flexion angle, the program translated the femur in 1mm increments, from the 8mm anterior position through the 35mm posterior position. At each translated position, the femur was rotated about the global z-axis, through a range from 18° external to 10° internal, in 2° increments. Following these initial movements, it was necessary to compute the minimum distance between the femur and tibia. However, as the known femur points were not necessarily aligned over known tibial coordinates, this distance computation required the development of a separate algorithm.

a. Distance Algorithm

The algorithm for computing the minimum separation distance between the femur and the tibia required the projection of each femur point onto the global x-y plane. Distances between this point and every tibial point were computed and sorted. Initially, the three most proximal tibial points were utilized to construct a grid and the x-y coordinates of the femur point were evaluated to ascertain if they fell within the grid of those three points (Figure 15). If they did not, then the next most proximate tibial point was checked and the femur coordinates were reevaluated (Figure 16). Once appropriate

points were identified, the equation of their plane was computed and the z coordinate of the tibial point that corresponded with the x and y coordinates of the femur point was calculated. The difference between the femur point's z coordinate and this computed tibial z coordinate provided the separation distance between the femur and tibia. This process was repeated for each femur point, thus providing a measure of separation between each known femur point and the tibia.

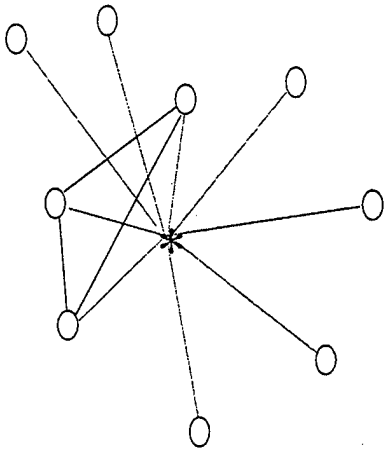

Figure 15. Evaluating Most Proximate Tibial Points for Plane Determination.

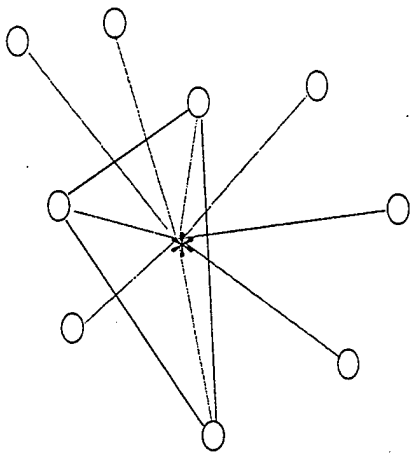

Figure 16. Evaluating Next Most Proximate Tibial Point for Plane Determination.

b. Achieving Stability: Contact in both Condyles

After completion of this algorithm, the femur was displaced distally by the minimum separation distance; this resulted in a single point of contact between the tibial and femoral surfaces. However, a stable knee is one in which there is contact in both condyles. Therefore, to achieve stability, the femur was rotated in the x-z plane, about

the contact point, until contact in both condyles was achieved (Figure 17). Contact was defined as the bone surfaces being within .01 mm of each other.

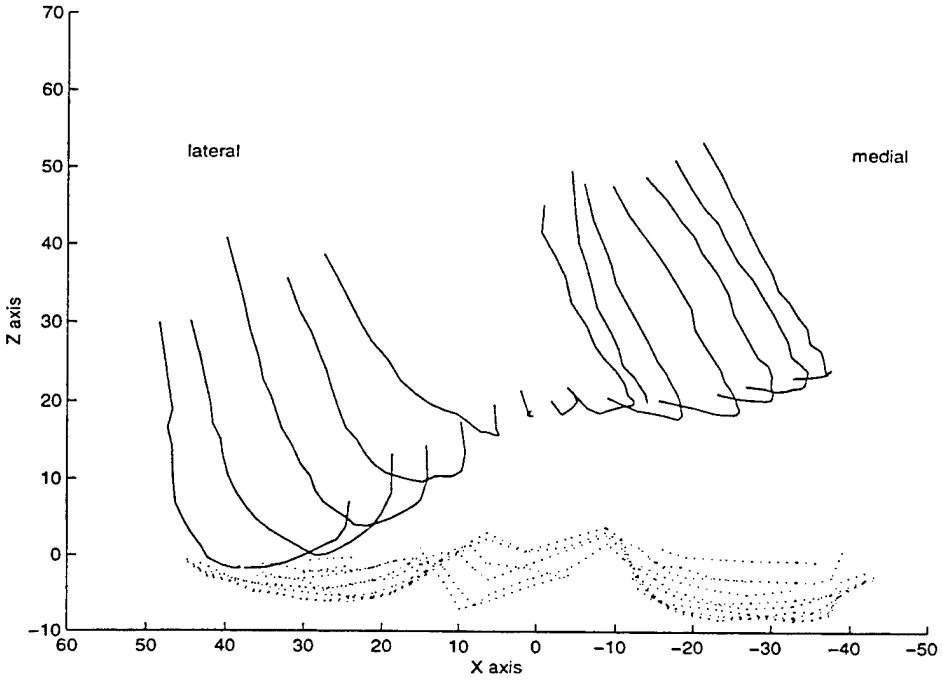

Figure 17. Contact in a Single Condyle. Contours of femoral and tibial surfaces are represented as previously described.

The required x-z plane rotation was accomplished through a bifurcation algorithm. The subroutine was designed to measure, in each condyle, the minimum directed distances between the surfaces. Due to the irregularity of the bone surfaces and the importance of these surfaces as a constraint to motion, it was not permissible to approximate the "required angle of rotation"; the separation distance had to be computed at every rotation. Initially, the femur was rotated about its contact point at an angle chosen to result in the femur "passing through" the tibia (Figure 18). This established an upper bound on the rotation angle. Computation of the minimum separation distance in

each condyle provided the basis for determining if the rotation angle needed to be increased or decreased for the next rotation.

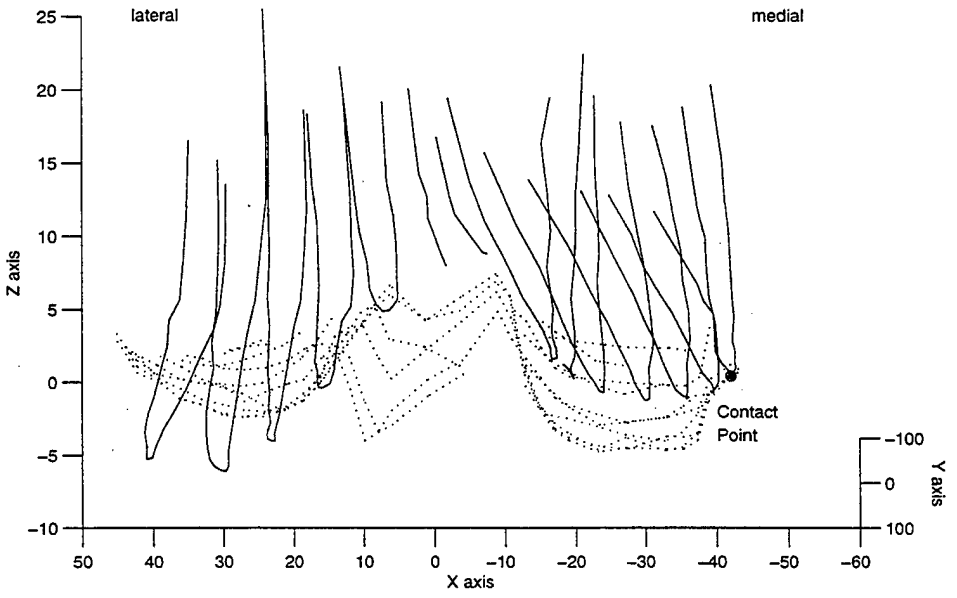

Figure 18. Rotation of Femur to Produce Tibial "Pass Through". Contours of femoral and tibial surfaces are represented as previously described.

On occasion, the rotation angle converged without the surfaces achieving contact in both condyles. When the angle did not change by more than 3.5e-5 degrees between rotations, the contact point was redefined. The femur point chosen as the new contact point was the one whose directed separation distance was the least negative i.e., the point which "passed through" the tibia by the least amount.

C. COMPUTATION OF POTENTIAL ENERGY

As previously mentioned, the "system" addressed in this model consists of the four major ligaments of the knee: the lateral collateral, medial collateral, anterior cruciate and posterior cruciate ligaments. Utilizing the experience of Crowninshield, each cruciate ligament was further modeled as two separate ligament elements, one anterior, one posterior [Ref. 1:p. 398]. Paralleling Essinger's choice to utilize Wismans' quadratic force-elongation function, each element was modeled as a non-linear spring whose potential energy is given by:

$$PE_i = \frac{1}{3} k_i (\Delta l_i)^3 (a_i) \qquad (1)$$

where Δl_i is the change in length of a ligament from the length in the fully extended position and is measured in mm. The spring constant of a ligament, k_i, is measured in N/mm^4 [Ref. 2:p. 1231] and a_i, the relative cross-sectional area of that ligament, is measured relative to the cross-sectional area of the anterior fiber of the medial collateral ligament [Ref. 1:p. 398]. The spring constants and relative areas utilized are depicted in Table 1.

LIGAMENT	SPRING CONSTANT (N/mm^4)	RELATIVE AREA
Lateral Collateral	18	.5
Medial Collateral	16	.75
Anterior Fiber of Posterior Cruciate	12	.8
Posterior Fiber of Posterior Cruciate	13	.8
Anterior Fiber of Anterior Cruciate	19	.5
Posterior Fiber of Anterior Cruciate	20	.5

Table 1. Ligament Spring Constants and Relative Areas from Refs. [2] and [1], respectively.

The potential energy of the system of six ligaments is the sum of the potential energy of each element. However, unlike a spring, ligaments are resistive to only tensile forces. Therefore, whenever a position was reached in which a ligament underwent contraction, the resultant potential energy for that ligament, was set to zero.

The determination of the position of the femur in each of the 7920 orientations inherently determined the position of the ligament attachment sites. From these positions, the extension or contraction of each ligament was computed, from which the potential energy of each ligament and the system were calculated.

D. PRETENSIONING

The original simulation was based upon the assumption that the ligament was undergoing no compression or tension at the position of full extension; i.e., at that position there was no pretensioning of the ligaments. The length of the ligaments at this position provided the reference for computation of ligament contraction or extension during subsequent movement of the femur. However, as shown in Table 2, Essinger, Crowninshield and Wang have shown that all ligaments are not at their minimum length at the position of the full extension [Refs. 1, 2 and 9, respectively]. To account for this, each ligament length at the position of full extension was multiplied by its respective

	Essinger	Crowninshield	Wang
Lateral Collateral	.95	.84	.75
Medial Collateral	1.0	.94	.83
Anterior Fiber PCL	.95	.97	.91
Posterior Fiber PCL	.94	.8	1.14
Anterior Fiber ACL	.95	.96	.89
Posterior Fiber PCL	.975	1.0	.91

Table 2. Minimum Ligament Length Relative to Length at Full Extension from Refs [2], [1] and [9], respectively.

minimum length ratio. The new, shorter lengths were utilized as the basis for determining the extension or contraction of the ligaments in the 7920 orientations of the femur.

As shown in Table 1, there is considerable variability between the results of the researchers; this may be the result of the individuality of the specimens examined and the number of samples. Because the initial choices in the development of this thesis utilized the ligament attachment sites and relative cross-sectional areas from Crowninshield's research, Crowninshield's ligament length ratios were also selected to ensure consistency. These new minimum ligament lengths imply an elongation of the ligaments at the position of full flexion, indicating that the ligaments are under tension at the position of full extension. The adjectives pretensioning and pretensioned will be used throughout the remainder of this thesis whenever Crowninshield minimum length ratios are utilized. This will assist in distinguishing these results from those which used the original, fully extended ligament length as the reference for determining ligament extension or contraction.

E. ACL AND PCL DEFICIENT MODELS

To examine the effect of an ACL deficient knee, the simulation was run with all ACL ligament lengths, those in the fully extended and flexed positions, set to zero. This provided the opportunity to examine the effect that a ruptured ACL has on the path of minimum strain energy. To evaluate the motion of a PCL deficient knee, the simulation was run with all PCL ligament lengths set to zero. Both ACL and PCL deficient knees were investigated with the pretensioned ligament length ratios applied.

III. RESULTS

In this chapter, the results of the simulation and previous research presented. On the surface, there appears to be significant variation between the results of the research in this field. In experimental investigations, reasons for this may be due to both the individuality of the tested samples and the number of samples utilized. For both experimental and theoretical studies, the lack of a common reference frame also contributes to the difficulty in comparing results achieved by different researchers. Nevertheless, where available, the results of previous studies are presented.

A. POTENTIAL ENERGY CURVES

For each 10° increment of flexion, the simulation computed the potential energy of the six ligament system at 660 different femur orientations. Graphing these results utilizing a cubic spline interpolation produces a potential energy plot over an infinite range of orientations. Figure 19 is an example of such a plot; it is a map of the total potential energy for a non-pretensioned femur in 10° of flexion. In this graph, as in subsequent plots of potential energy, both internal rotation (IR) and anterior translation (A) are represented as positive quantities on their respective axis; external rotation (ER) and posterior translation (P) are negative quantities. As all of the potential energy curves reflect a similar growth of potential energy at large posterior translations, only significant portions of the graphs are depicted in subsequent potential energy maps. The graph allows the position of the femur that results in the least storage of strain energy to be deduced.

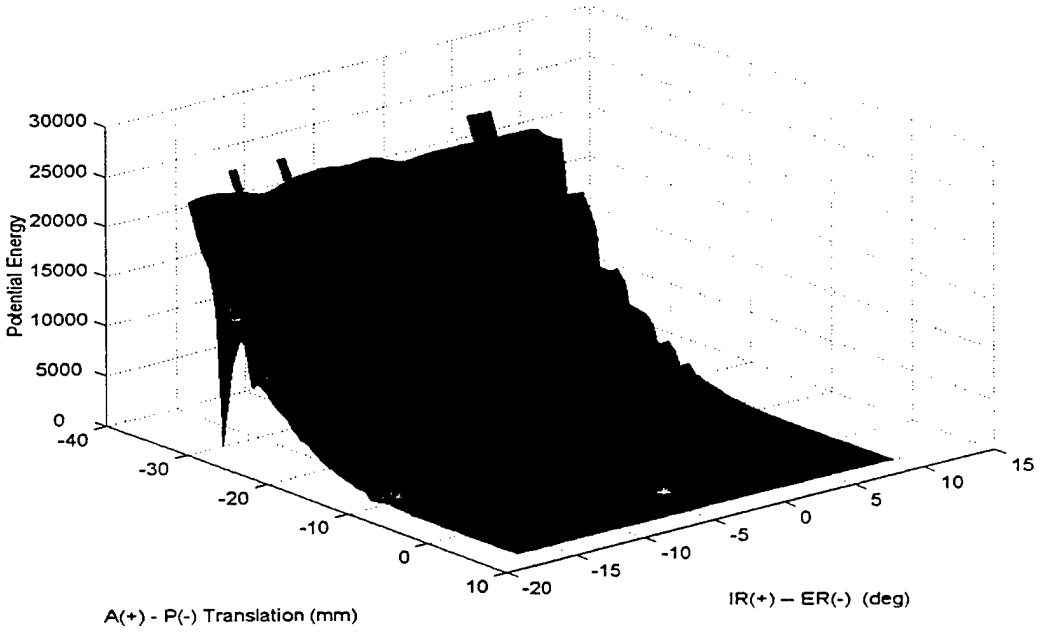

Figure 19. Potential Energy Map for 10° of Flexion

1. Without Pretensioning

Figures 20 through 23 depict the potential energy curves for each 30° increment of flexion, when pretensioning of the ligaments is assumed to be zero.

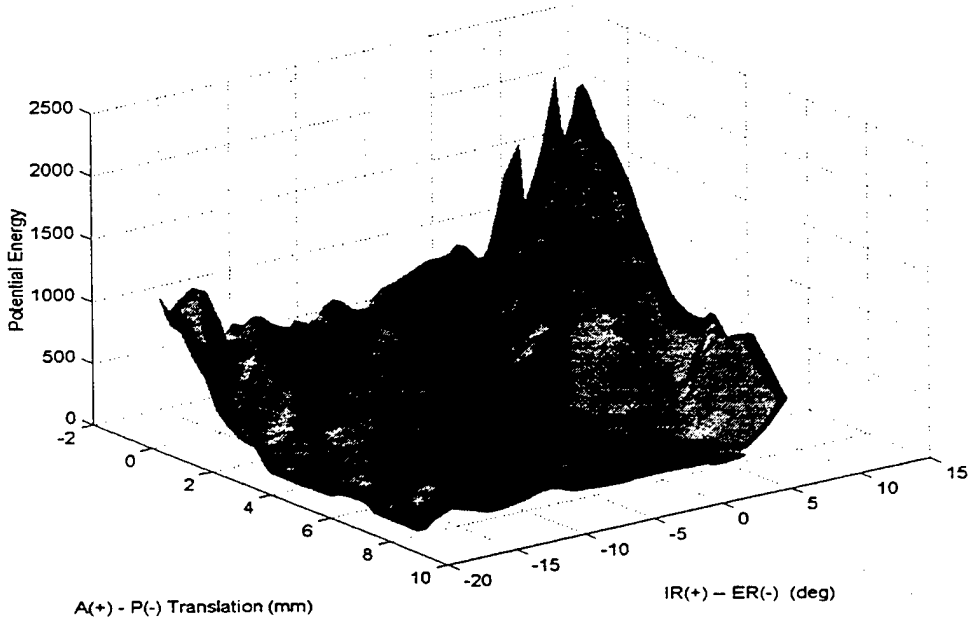

Figure 20. Potential Energy Map for 30° of Flexion

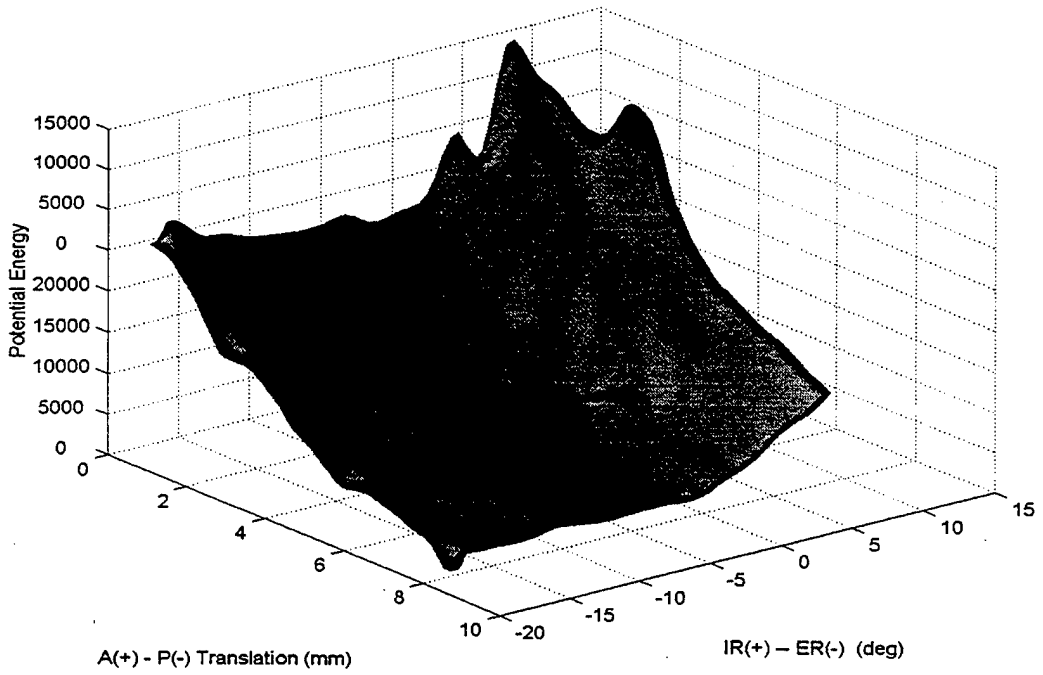

Figure 21. Potential Energy Map for 60° of Flexion

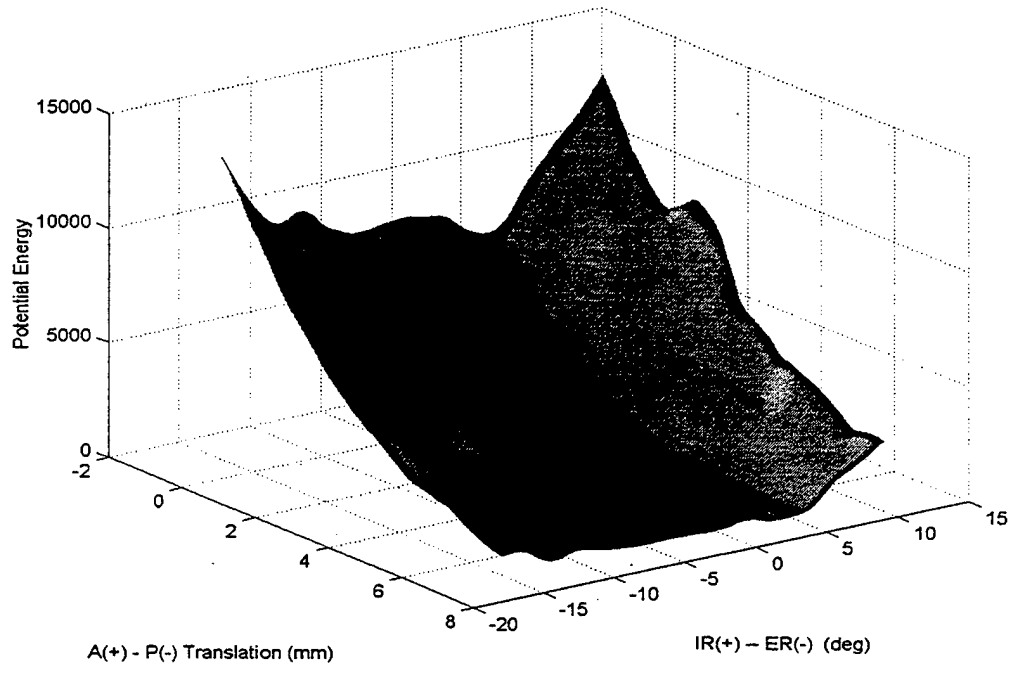

Figure 22. Potential Energy Map for 90° of Flexion

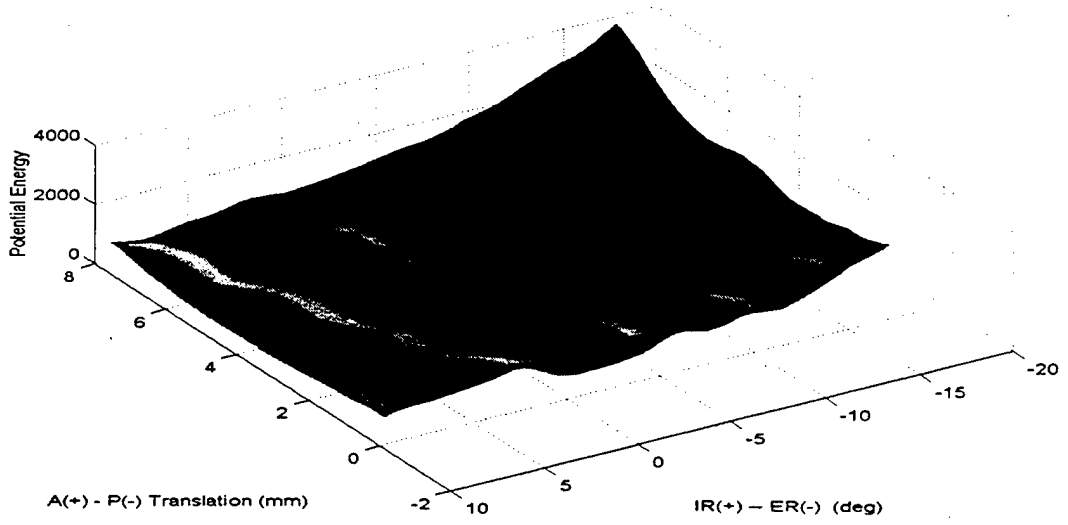

Figure 23. Potential Energy Map for 120° of Flexion

2. Pretensioned Ligaments

As explained previously, if the shortest length of each ligament does not occur at the position of full extension, the ligament is undergoing tensile forces at the position of 0° flexion. The work done by Essinger [Ref. 2:p. 1234], Crowninshield [Ref. 1:p. 400], Wismans [Ref. 3:p. 684] and Wang [Ref. 9:p. 589-592], have each demonstrated that not all of the cruciate and collateral ligaments are shortest at the position of extension, as was shown in Table 2. When the Crowninshield ligament length ratios were applied in the calculations of potential energy, different potential energy maps result; the salient portions of these maps are depicted in Figures 24 through 27, for each 30° of flexion.

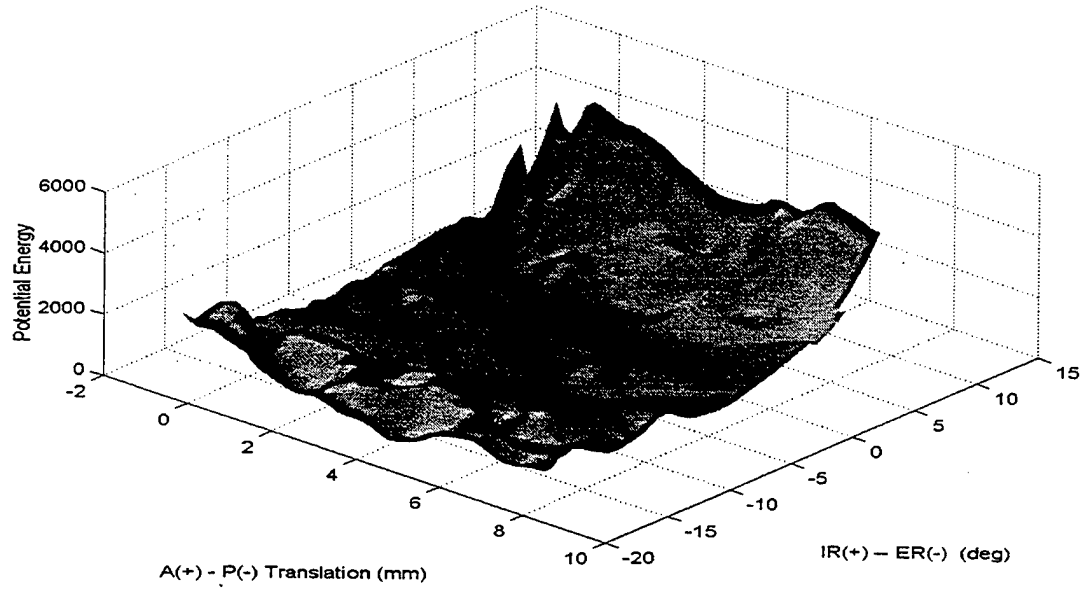

Figure 24. Potential Energy Map for 30° of Flexion with Pretensioning

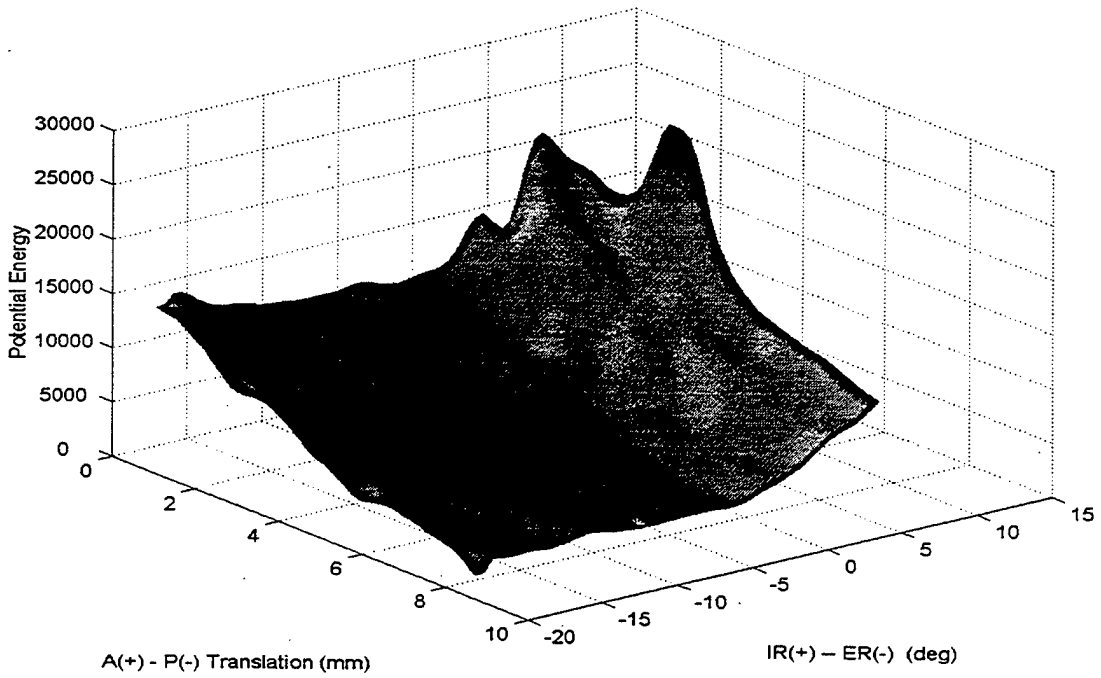

Figure 25. Potential Energy Map for 60° of Flexion with Pretensioning

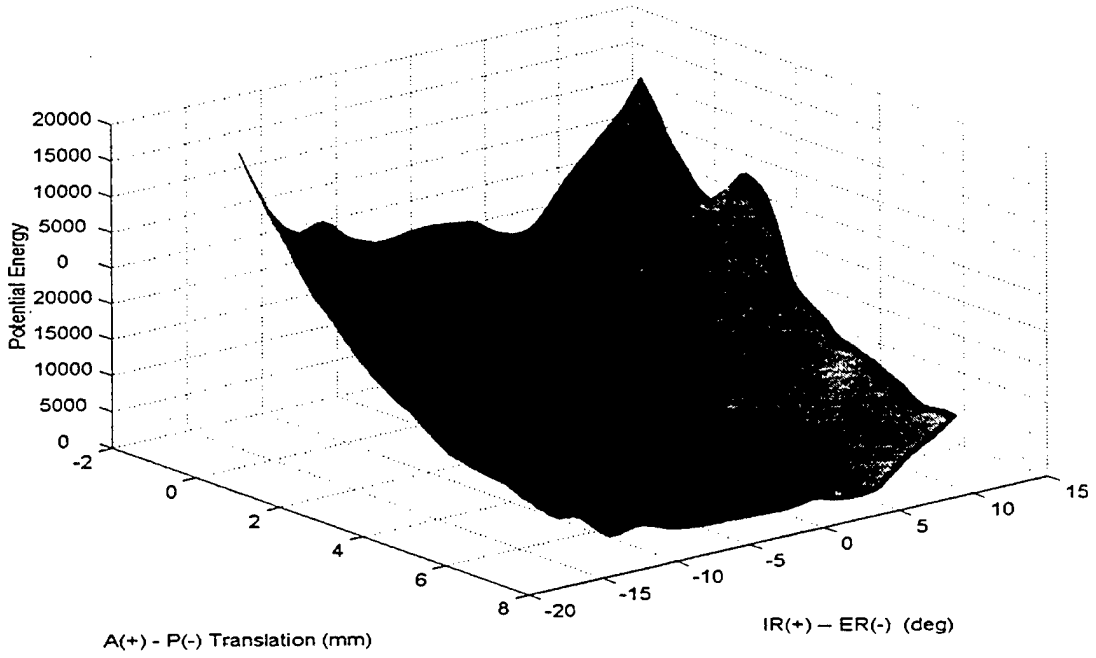

Figure 26. Potential Energy Curve for 90° of Flexion with Pretensioning

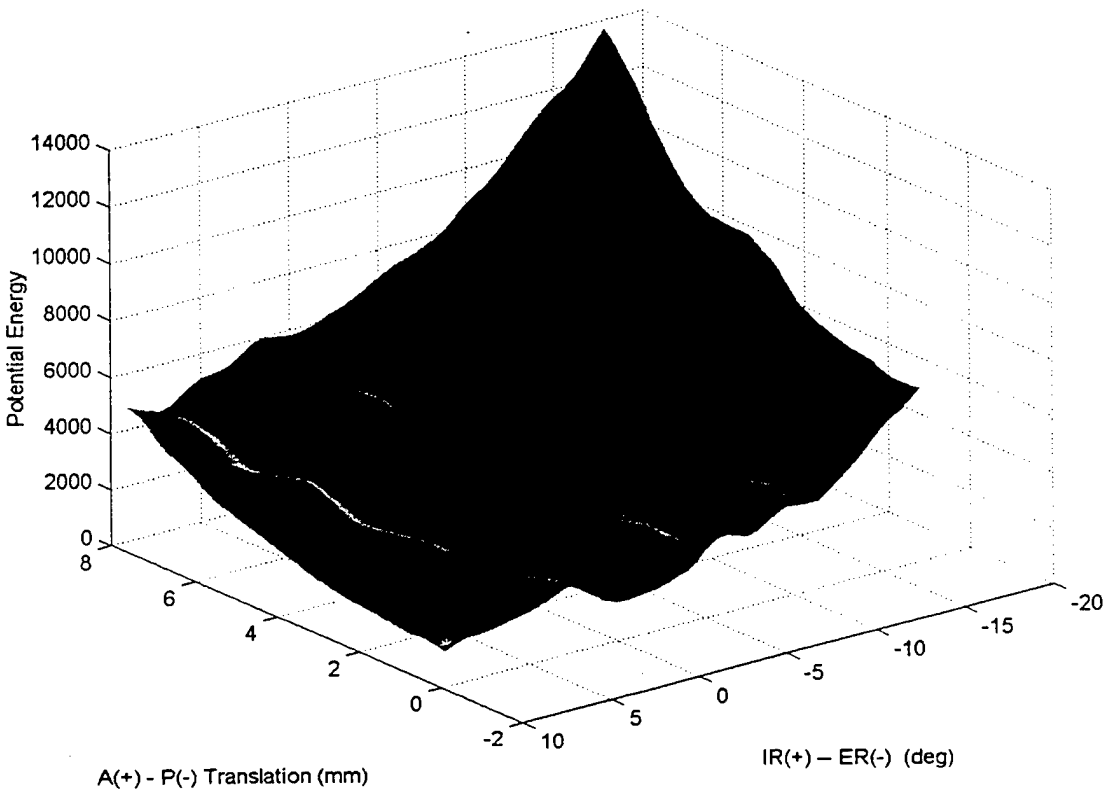

Figure 27. Potential Energy Curve for 120° of Flexion with Pretensioning

3. ACL Deficient

If the anterior cruciate ligament is damaged, the motion of the femur will change, resulting in new potential energy curves for each flexion increment. These curves, representing an ACL deficient knee, are depicted in Figures 28 through 31.

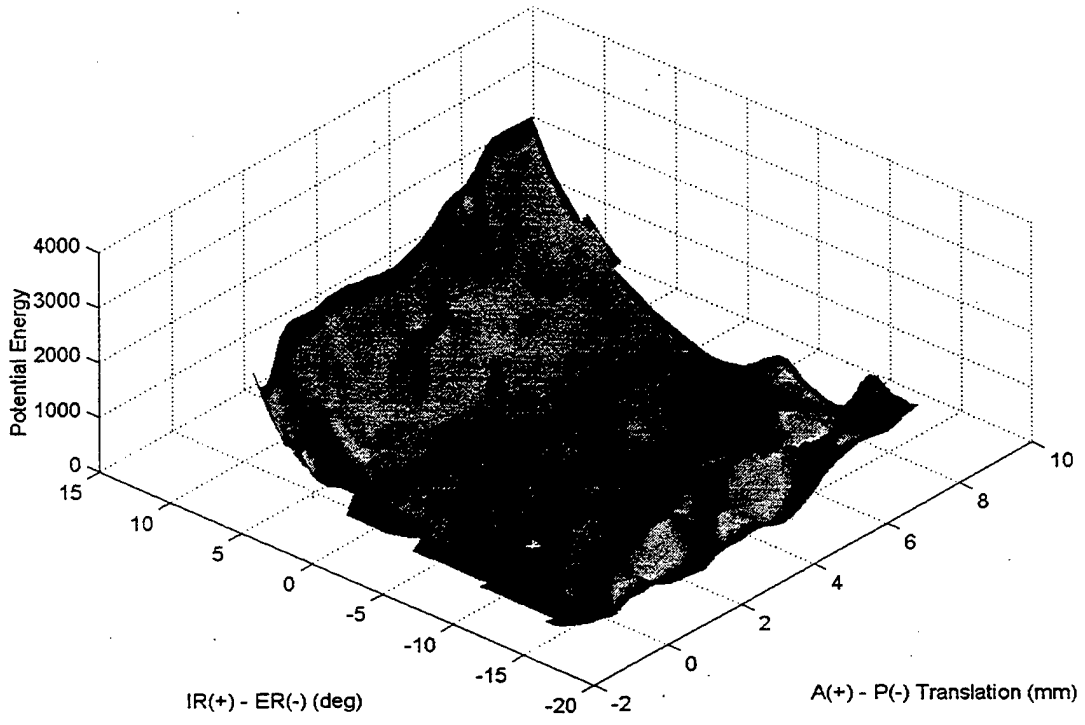

Figure 28. Potential Energy Map for 30° of Flexion for ACL Deficient Knee

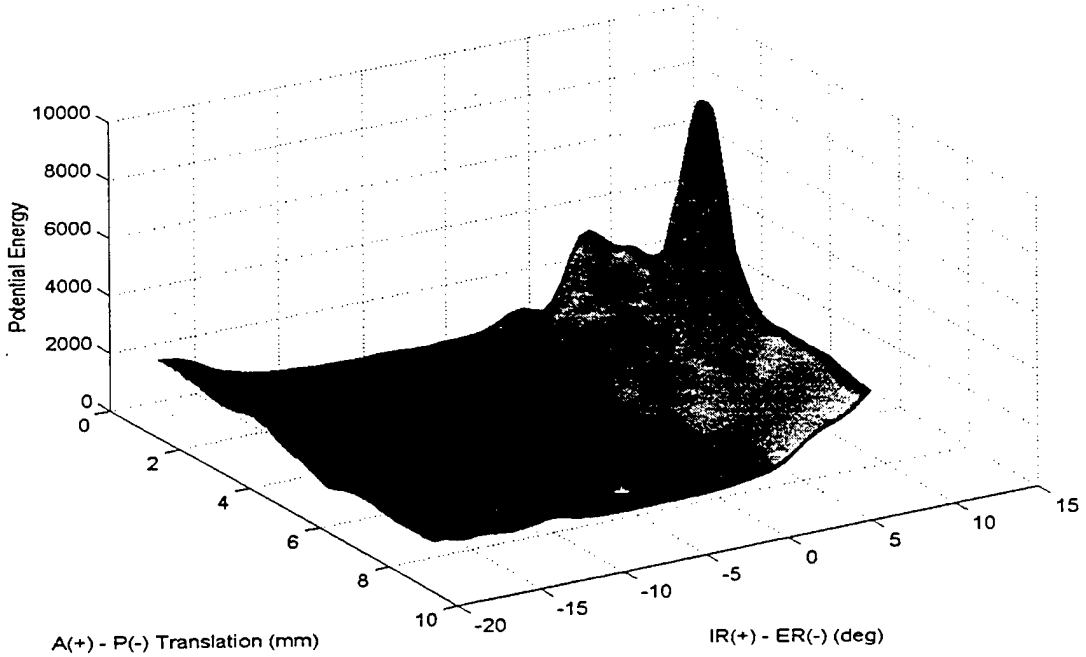

Figure 29. Potential Energy Map for 60° of Flexion for ACL Deficient Knee

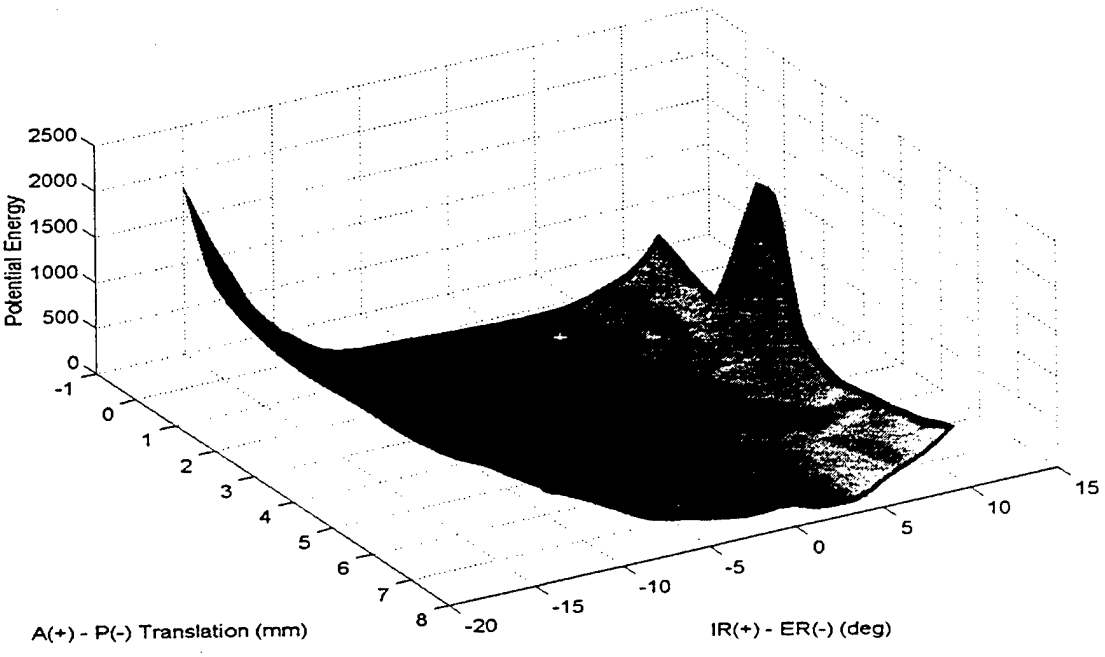

Figure 30. Potential Energy Map for 90° of Flexion for ACL Deficient Knee

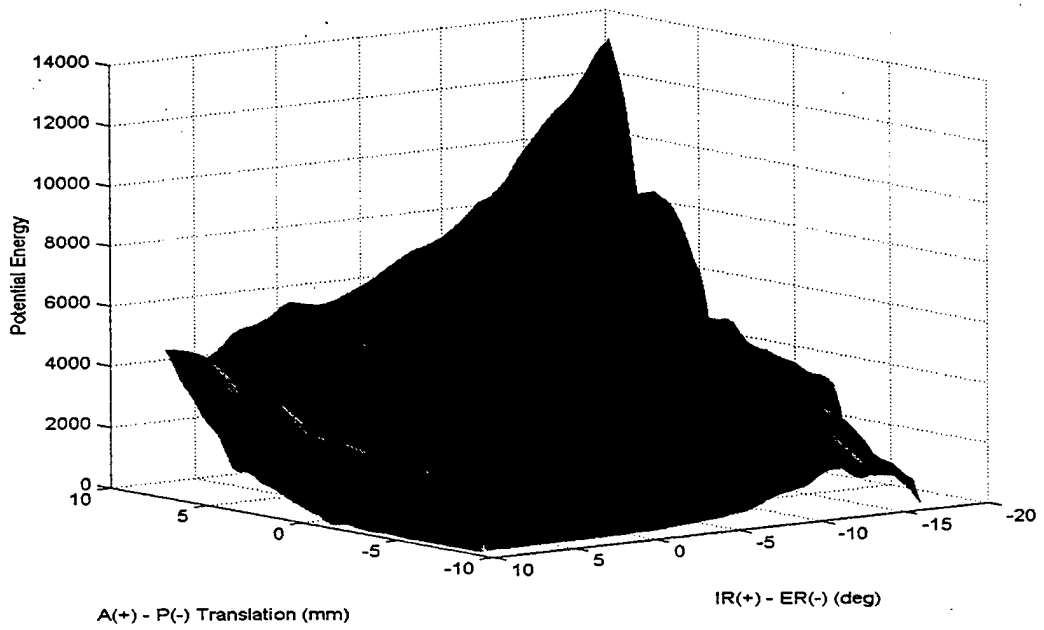

Figure 31. Potential Energy Map for 120° of Flexion for ACL Deficient Knee

4. PCL Deficient

Similarly, if the posterior cruciate ligament is damaged, the motion of the femur will change, resulting in new potential energy curves for each flexion increment. These curves are depicted in Figures 32 through 35.

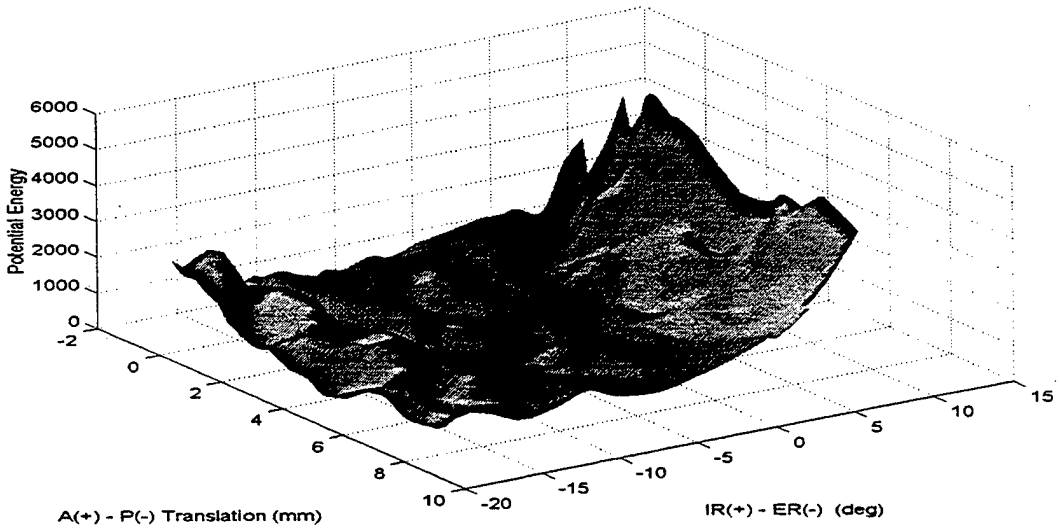

Figure 32. Potential Energy Map for 30° of Flexion for PCL Deficient Knee

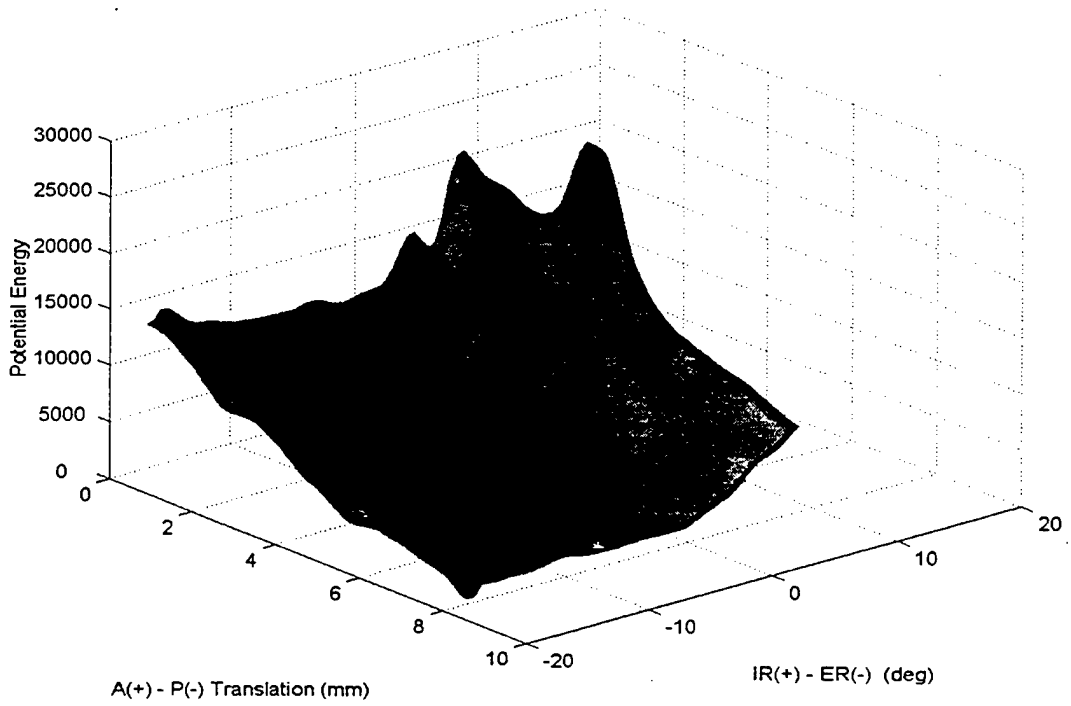

Figure 33. Potential Energy Map for 60° of Flexion for PCL Deficient Knee

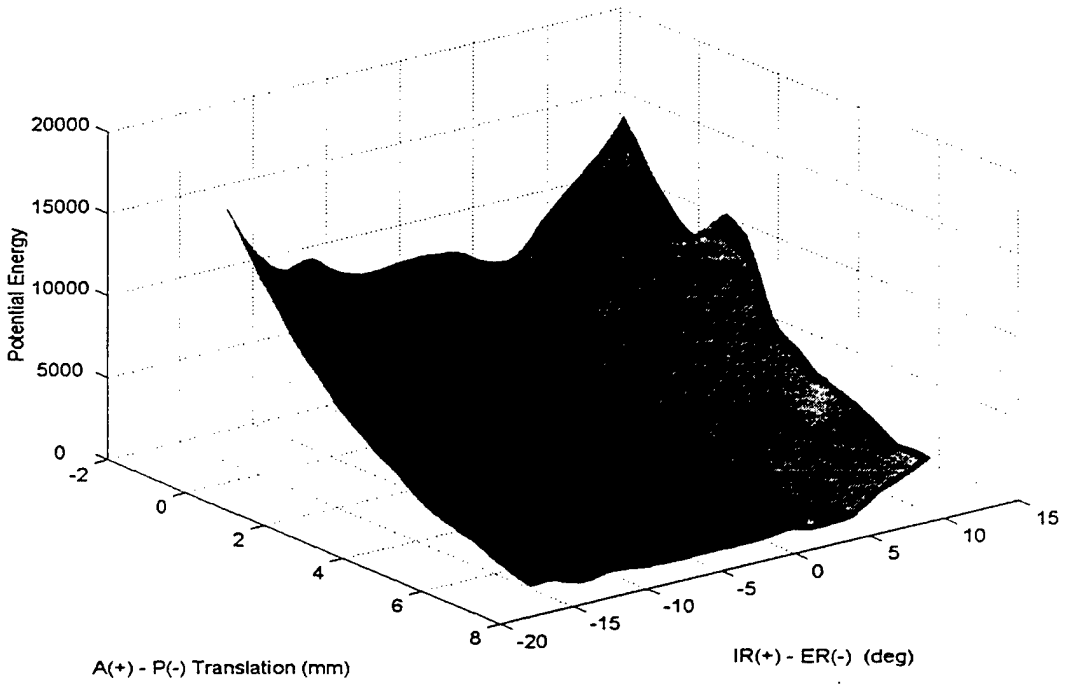

Figure 34. Potential Energy Map for 90° of Flexion for PCL Deficient Knee

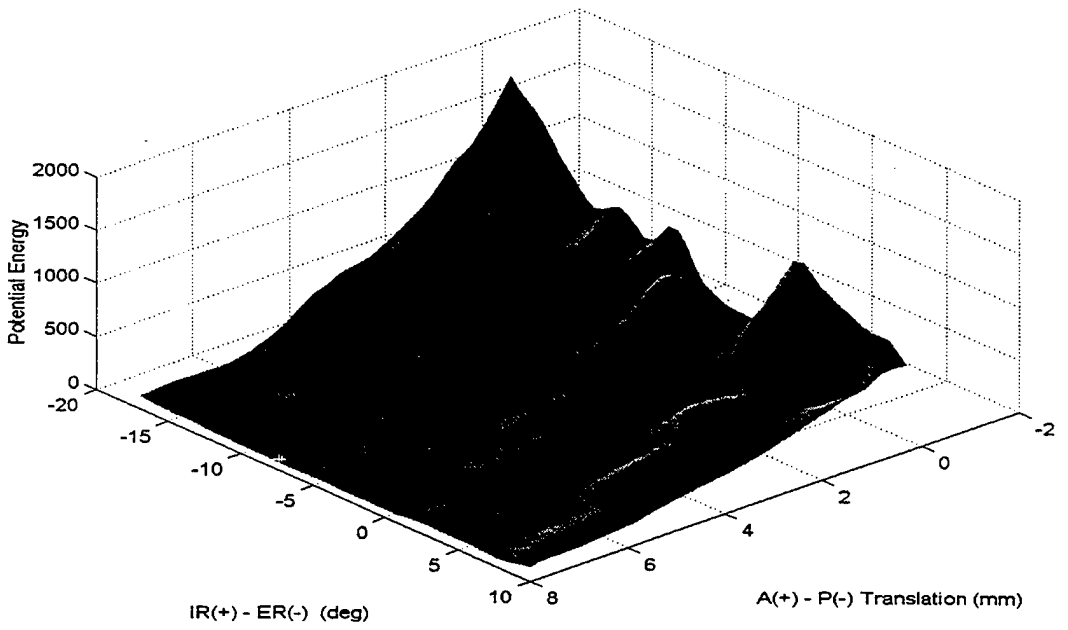

Figure 35. Potential Energy Map for 120° of Flexion for PCL Deficient Knee

B. FEMUR ORIENTATION THROUGHOUT FLEXION

By mathematical assessment of the potential energy curves, it is possible to determine, for every degree of flexion, the orientation of the femur that results in the minimum potential energy. From these positions, the translation and rotation of the femur during flexion through 120° can be investigated.

1. Proximal-Distal and Anterior-Posterior Translation

a. Previous Research

Essinger found the total proximal-distal translation was less than 2.5 mm, with 80% of this motion occurring within the first 15° of flexion [Ref. 2:p. 1235]. Figure 36 depicts Essinger's computational results graphically. Kurosawa found that the lateral center of the femur translated distally by 3mm from 0-30° of flexion with both the

medial and lateral centers of the femur translating 1mm distally, from 30°-120° [Ref. 10:p. 494].

In Kurosawa's analysis of cadaver knees, he found that the medial center translated a total of 4.5 mm anteriorly, followed by 2.3mm anterior translation [Ref. 10:p. 494]. The center of the lateral femoral condyle moved back a total of 17 mm, at a rate which decreased with increasing flexion [Ref. 10:p. 494]. The volunteers whom he studied showed an anterior movement of the medial center by 4.4 mm, followed by a posterior movement to a final distance of 0.3mm [Ref. 10:p. 496]. The lateral condylar center moved steadily posteriorly to an average of 14mm at 120° [Ref. 10:p. 496]. Figure 37 depicts the Kurosawa's anterior-posterior translation results from observations and analysis of cadaver knees.

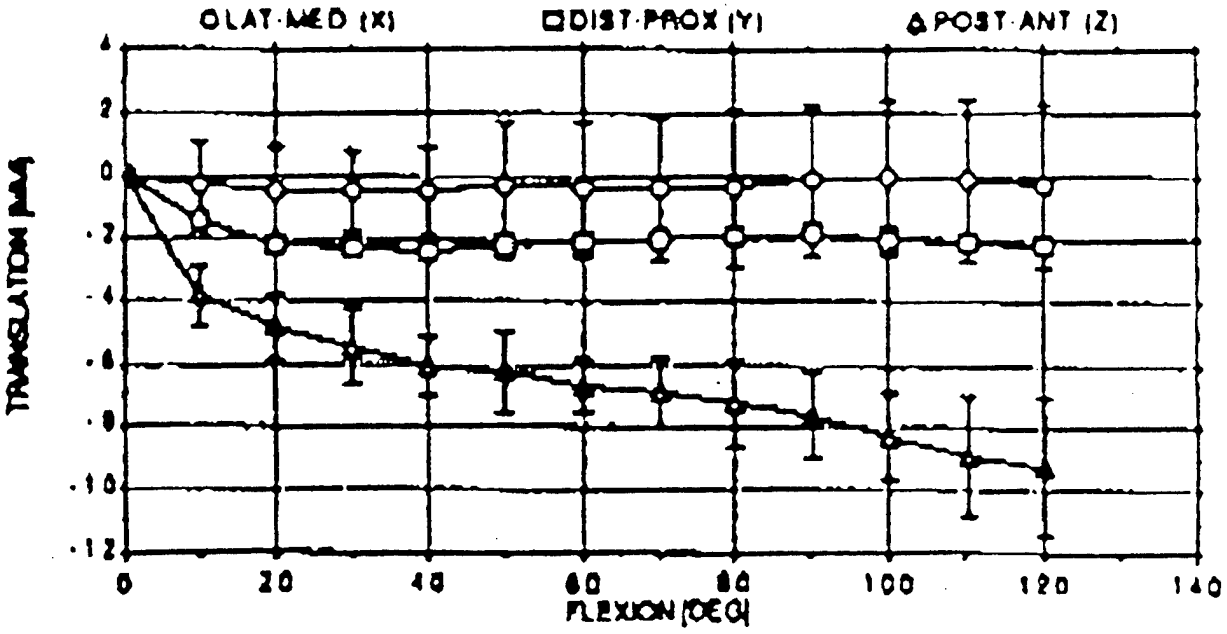

Figure 36. Essinger's Translation Results

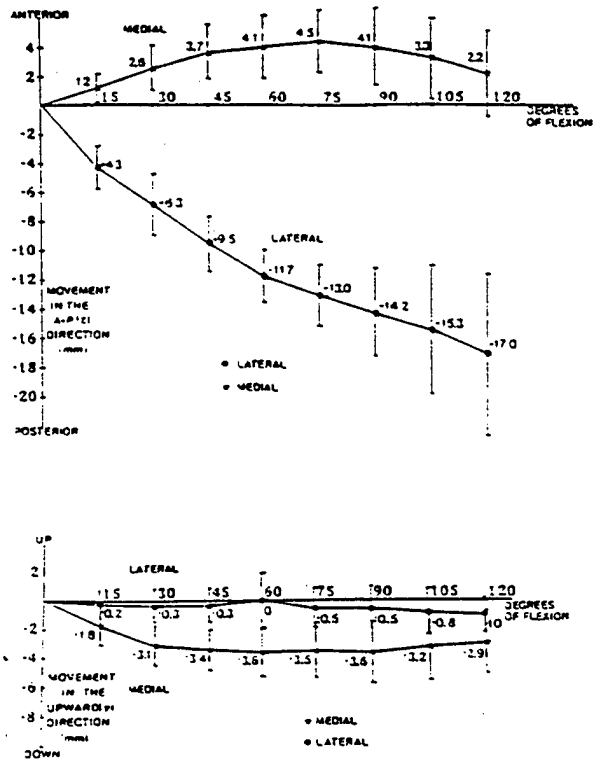

Figure 37. Kurosawa's Translation Results

b. Simulation Results (No Pretensioning)

Table 3 depicts the translations of the femur when there is no assumed ligament pretensioning; these results are graphed in Figure 38. The medial condyle reference point reached a maximum forward translation of approximately 18mm at about 47° of flexion. Although it retained an anterior translation throughout flexion, there were 8 inflection points, points during which the medial condyle would move opposite to its previous direction. The lateral condylar reference point initially moved behind its position in full extension, then moved forward, only to return to a posterior position during flexion from 25° to 52°, after which it remained forward of its initial position. The lateral condyle showed 10 different changes in movement direction.

Neither Essinger's nor Kurosawa's work showed these directional changes. Figures 39 through 42 display the position of x-axis of the femur for each 10° increment of flexion.

FLEXION	ANTERIOR(+)-POSTERIOR(-) (mm)	PROXIMAL(+)-DISTAL(-) (mm)
10°	2	.60
20°	5	2.10
30°	6	4.15
40°	8	7.49
50°	8	11.06
60°	8	14.83
70°	8	19.64
80°	8	23.97
90°	8	28.21
100°	8	32.65
110°	7	36.00
120°	4	38.73

Table 3. Femur Translation (No Pretensioning)

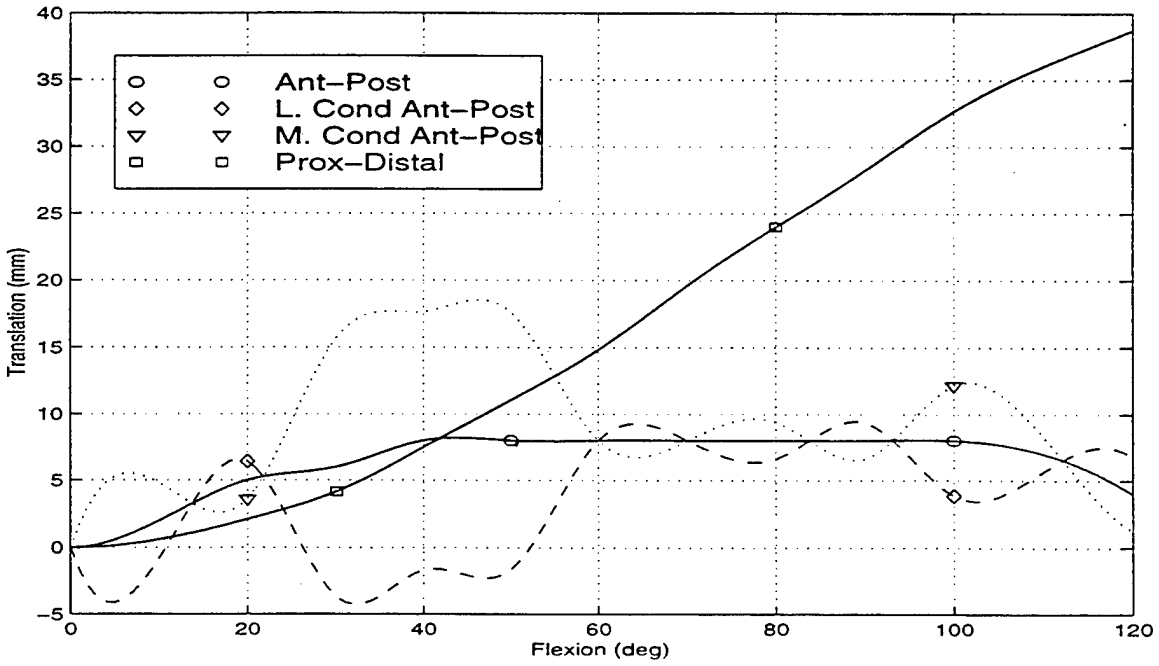

Figure 38. Femur Translation (No Pretensioning)

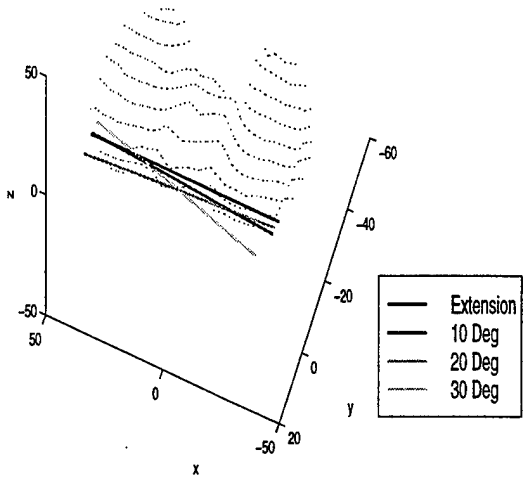

Figure 39. Femur X-Axis for 0°-30° of Flexion

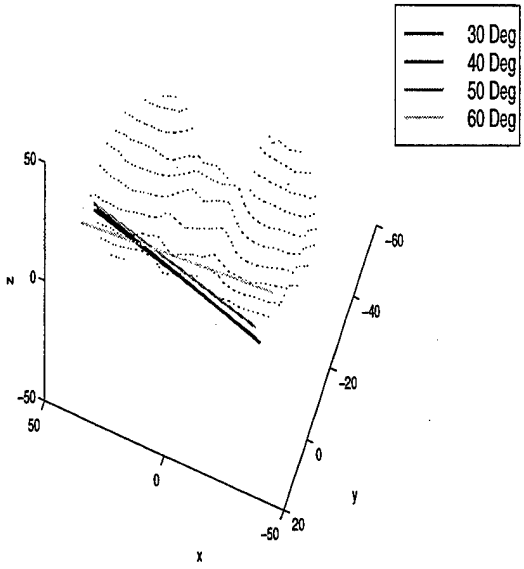

Figure 40. Femur X-Axis for 30°-60° of Flexion

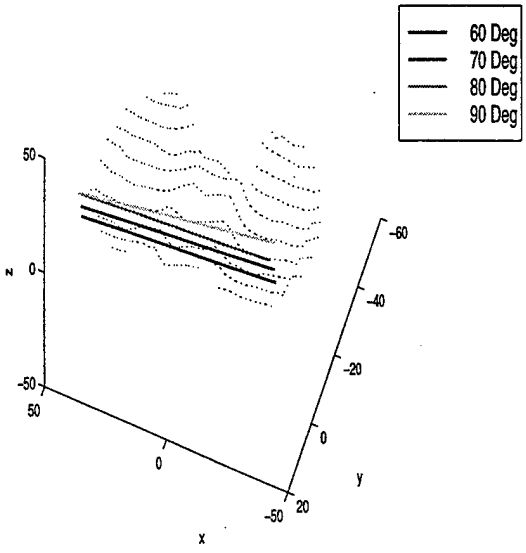

Figure 41. Femur X-Axis for 60°-90° of Flexion

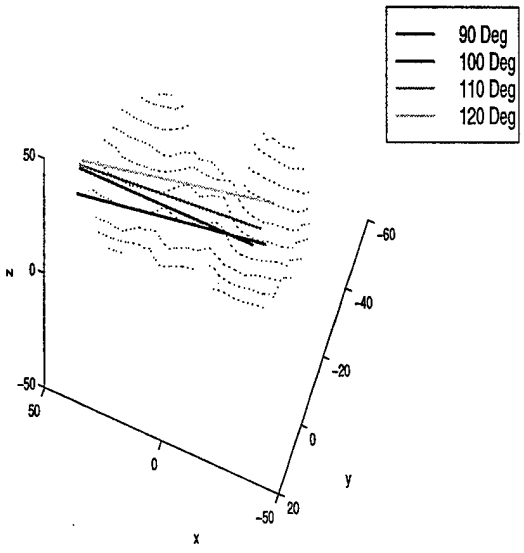

Figure 42. Femur X-Axis for 90°-120° of Flexion

c. Simulation Results (with Pretensioning)

Table 4 shows the proximal-distal and anterior-posterior translation of the femur when Crowninshield's pretensioning is applied. Figure 43 depicts these results graphically. Until reaching approximately 110°, the reference point on the medial condyle shows a forward translation, peaking at 13mm at 30° of flexion and decreasing thereafter. The lateral condylar point moved to a posterior position only through 35° after which it moved forward of its fully extended position. Until 85° of flexion, it was always posterior to the medial condyle. After 85°, the reference point of the lateral condyle moves anterior to the medial, reaching a maximum of 12mm at 114° of flexion. A comparison of the solid, anterior-posterior line in Figure 43 to the posterior-anterior graphs of Essinger and Kurosawa does reflect much correlation. Figures 44 through 45 show the movement of the x-axis of the femur.

FLEXION	ANTERIOR(+)-POSTERIOR(-) (mm)	PROXIMAL(+)-DISTAL(-) (mm)
10°	-3	-.64
20°	3	1.75
30°	5	4.04
40°	8	7.39
50°	8	11.02
60°	8	15.28
70°	8	19.64
80°	8	23.97
90°	8	28.21
100°	7	32.82
110°	4	35.41
120°	0	37.98

Table 4. Femur Translation (Pretensioning)

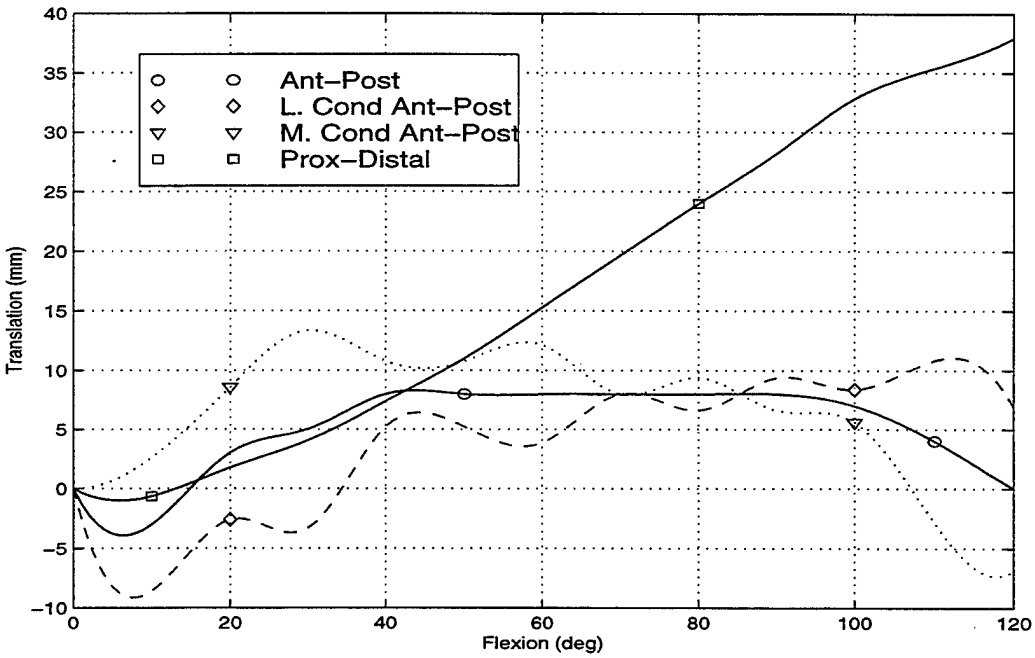

Figure 43. Femur Translation (Pretensioning)

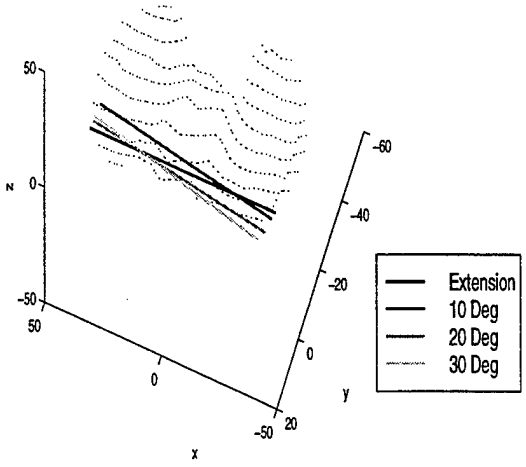

Figure 44. Femur X-Axis for 0°-30° of Flexion (Pretensioning)

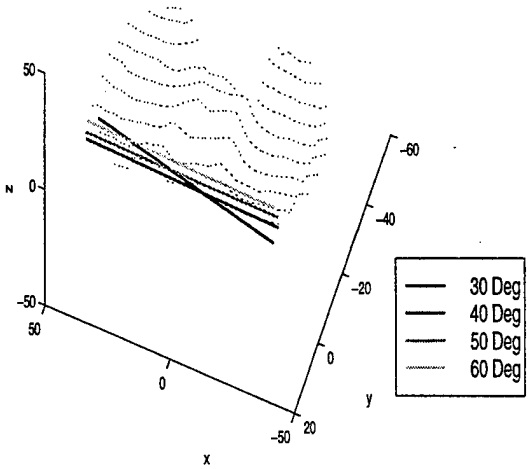

Figure 45. Femur X-Axis for 30°-60° of Flexion (Pretensioning)

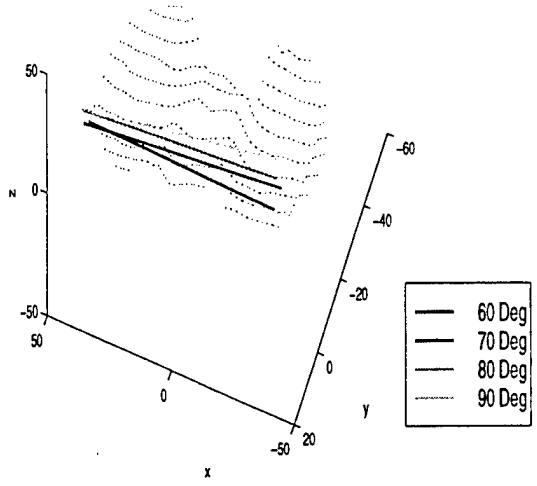

Figure 46. Femur X-Axis for 60°-90° of Flexion (Pretensioning)

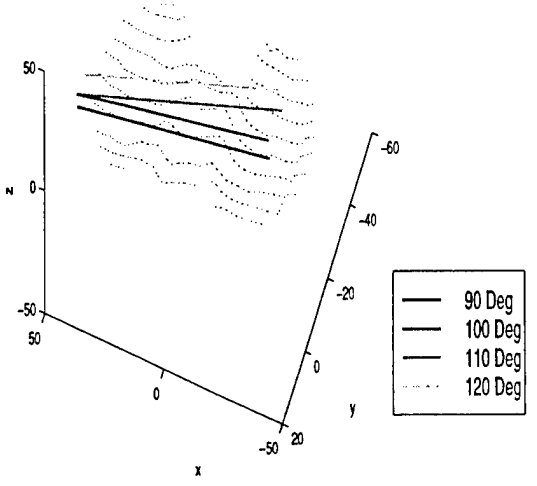

Figure 47. Femur X-Axis for 90°-120° of Flexion (Pretensioning)

d. Simulation Results for ACL Deficient Knee

Table 5 shows the translation of the femur during flexion from 0° through 120°, at the positions of minimum potential energy, for the ACL deficient joint. Figure 48 displays these results graphically. The motion of the x-axis of the femur is shown in Figures 49 through 52. As the ACL is the primary restraint to anterior motion of the tibia [Ref. 4:p. 154], the ACL deficient knee should exhibit increased posterior motion of the femur when compared with the intact, pretensioned joint. A comparison of fugures 43 and 48 show an increase in posterior motion of the femur, particularly in the earlier and latter stages of flexion. This would imply that the ACL plays a lesser role in stabilization during the middle stages of flexion, from 50° to 80°.

FLEXION	ANTERIOR(+)-POSTERIOR(-) (mm)	PROXIMAL(+)-DISTAL (-) (mm)
10°	-9	-1.40
20°	-3	.97
30°	1	3.64
40°	2	6.73
50°	7	10.75
60°	7	15.08
70°	6	19.39
80°	6	23.57
90°	1	27.84
100°	-3	31.59
110°	-3	34.63
120°	-9	37.24

Table 5. Femur Translation (ACL Deficient Knee)

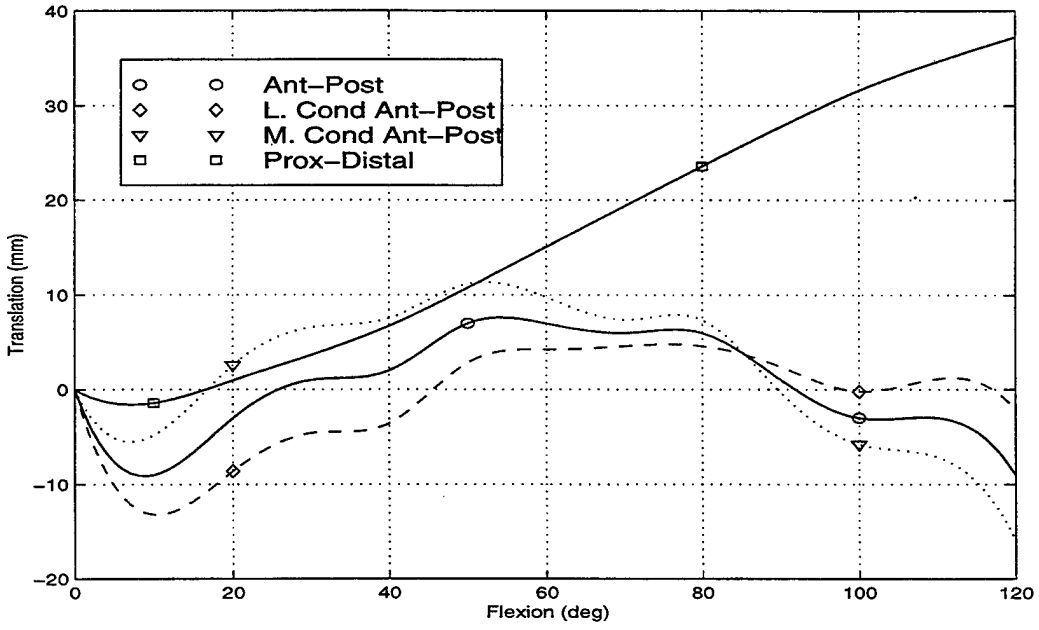

Figure 48. Femur Translation (ACL Deficient Knee)

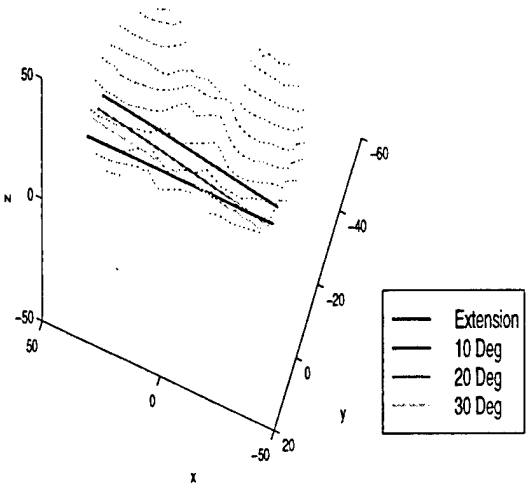

Figure 49. Femur X-Axis for 0°-30° of Flexion (ACL Deficient)

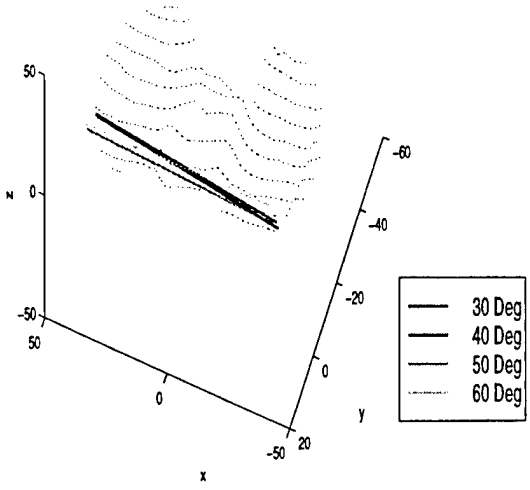

Figure 50. Femur X-Axis for 30°-60° of Flexion (ACL Deficient)

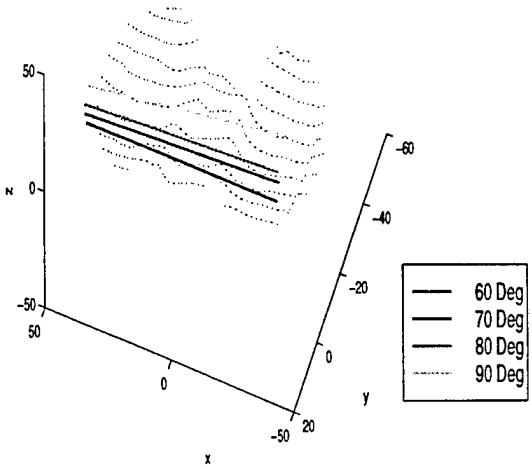

Figure 51. Femur X-Axis for 60°-90° of Flexion (ACL Deficient)

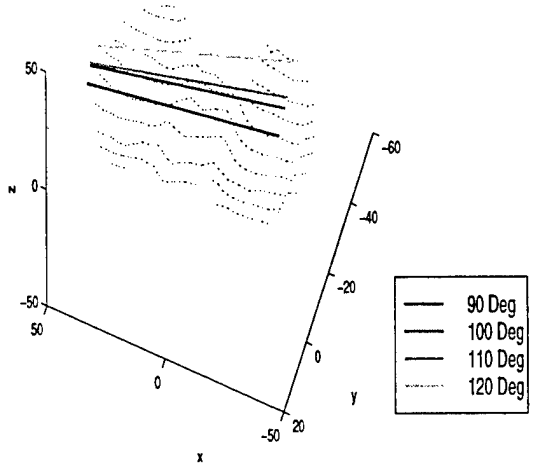

Figure 52. Femur X-Axis for 90°-120° of Flexion (ACL Deficient)

e. Simulation Results for PCL Deficient Knee

Table 6 shows the translation of the femur during flexion from 0° through 120°, at the positions of minimum potential energy for the PCL deficient case, with Crowninshield pretensioning applied. These are graphically depicted in Figure 53; the path of the femur x-axis is depicted in Figures 54 through 57. The PCL functions as the primary restraint to posterior displacement of tibia [Ref. 4:p 155]; therefore, without a PCL there should be increased posterior displacement of the tibia, or in the simulation reference frame, increased anterior displacement of the femur. This is shown by the simulation during flexion from 100° to 120°; a comparison of Figure 53 to Figure 43 shows greater anterior movement of the femur during this range of flexion in the PCL deficient, pretensioned knee than there is in the intact, pretensioned knee. This implies that the PCL plays a greater role during the latter stages of flexion.

FLEXION	ANTERIOR-POSTERIOR (mm)	PROXIMAL-DISTAL (mm)
10°	-3	-.63
20°	3	1.75
30°	5	4.03
40°	8	7.39
50°	8	11.02
60°	8	15.28
70°	8	20.04
80°	8	23.97
90°	8	28.21
100°	8	32.65
110°	8	36.54
120°	8	39.95

Table 6. Femur Translation (PCL Deficient Knee)

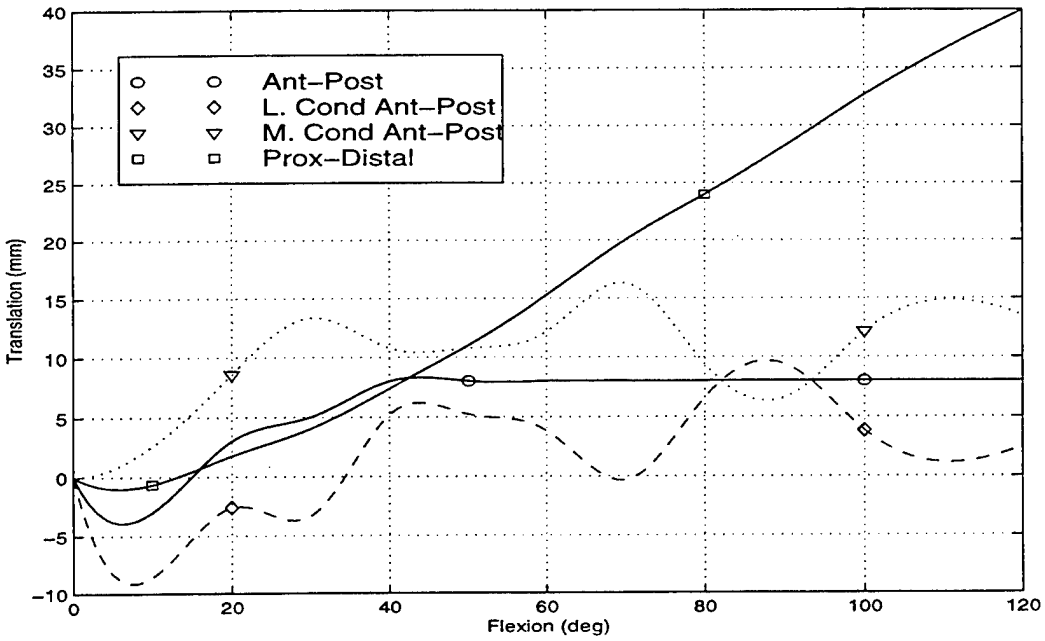

Figure 53. Femur Translation (PCL Deficient Knee)

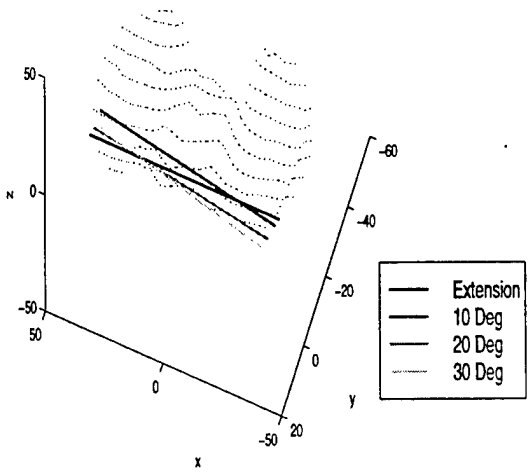

Figure 54. Femur X-Axis for 0°-30° of Flexion (PCL Deficient)

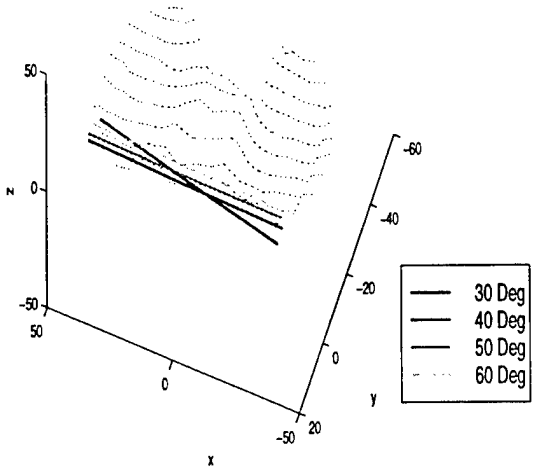

Figure 55. Femur X-Axis for 30°-60° of Flexion (PCL Deficient)

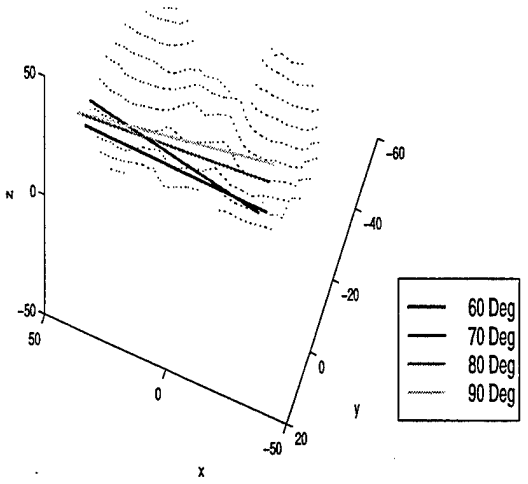

Figure 56. Femur X-Axis for 60°-90 of Flexion (PCL Deficient)

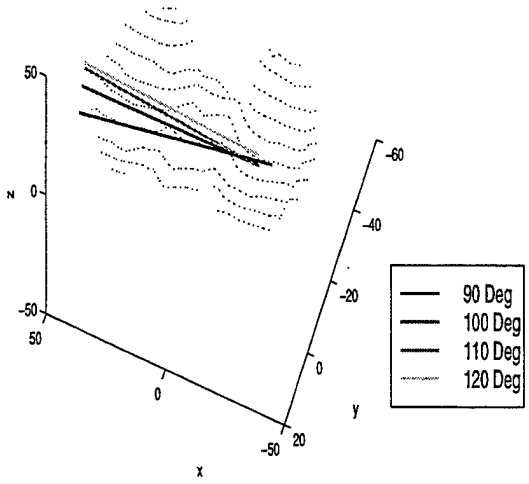

Figure 57. Femur X-Axis for 90°-120° of Flexion (PCL Deficient)

2. Internal-External and Varus-Valgus Rotation

a. Previous Research

Essinger found that the femur rotated externally an average maximum of 17° at 120 degrees of flexion, with approximately half of the rotation occurring within the first 18 degrees of flexion [Ref. 2:p. 1235]. In evaluating cadaver knees, Kurosawa found a maximum of 20.2° of external rotation, which peaked at 75° and then decreased [Ref. 10:p. 494]. His volunteers, however, showed an average maximum of 16.9° flexion that was achieved at 120° of flexion [Ref. 10:p. 496].

For varus-valgus rotation, Essinger found a maximum average value of 2° occurring at 50° of flexion and then decreasing to almost 0° at 120° of flexion [Ref. 2:p 1236]. Kurosawa found a greater degree of varus rotation, 4.2°, which occurred at

approximately the same degree of flexion, 45° [Ref. 10:p. 495]. Like Essinger, the amount of varus rotation then decreased, but only to 2.2°. Figures 58 and 59 display Essinger and Kurosawa's results, respectively. Note that Essinger uses an alternate rotational reference, measuring the tibia's rotation relative to the femur; his 'internal' tibial rotation corresponds to external femoral rotation.

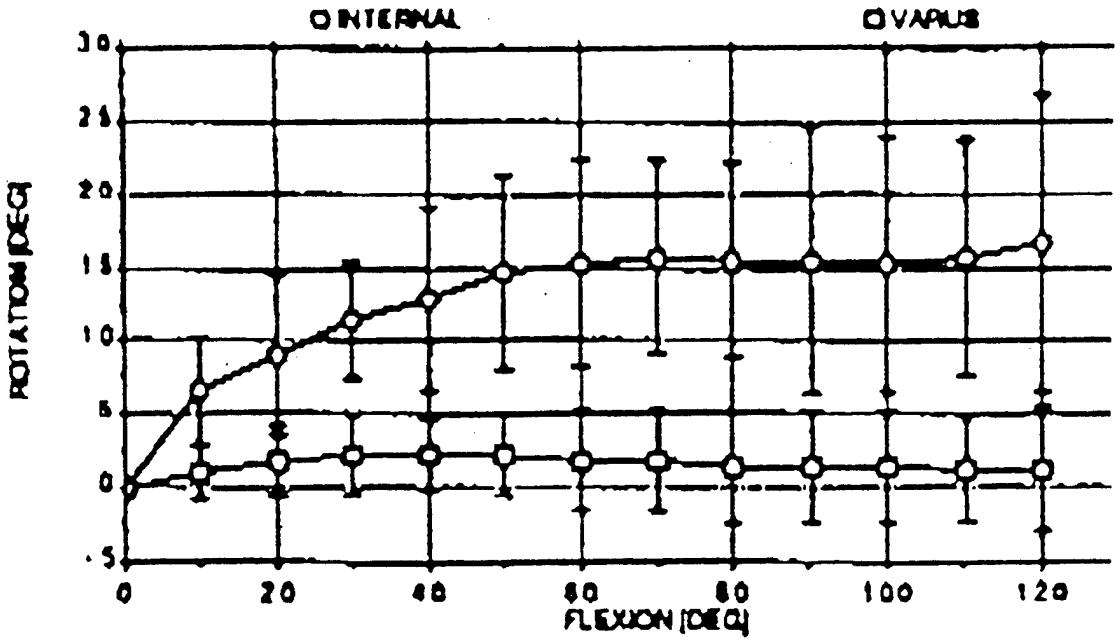

Figure 58. Essinger's Rotational Results from Ref. [2]

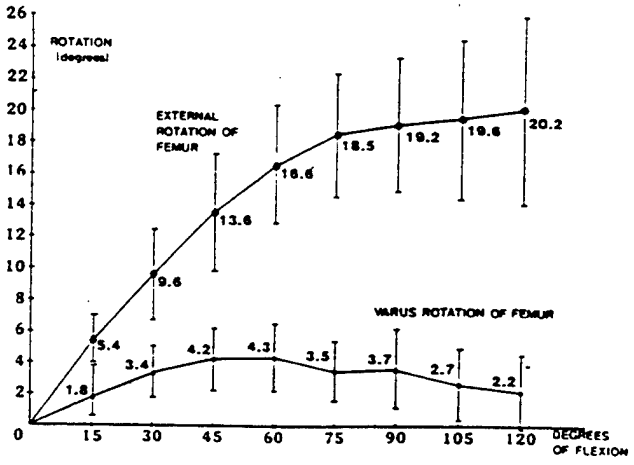

Figure 59. Kurosawa's Rotational Results from Ref. [10]

b. Simulation Results (No Pretensioning)

Table 7 depicts the internal-external and varus-valgus rotations of the femur with no pretensioning of ligaments. Figure 60 shows this graphically. The internal and external rotation can be deduced from the previous discussion of the translation of the lateral and medial reference points; just as those points undergo a change in relative position, so changes the rotation about the z-axis. Without accounting for pretensioning, the femur displays many changes in its orientation, changing between internal and external rotation seven times during flexion. Examining the varus-valgus rotation, without pretensioning, the simulation did not produce results similar to either Essinger or Kurosawa.

FLEXION	INTERNAL(+)-EXTERNAL(-) (deg)	VARUS(+)-VALGUS(-) (deg)
10°	-4.00	-1.86
20°	2.00	-1.00
30°	-14.07	-6.03
40°	-14.04	-7.55
50°	-14.04	-8.94
60°	0	-5.48
70°	0	-6.37
80°	-2.01	-8.27
90°	2.00	-7.55
100°	-6.06	-10.87
110°	0	-9.21
120°	3.99	-7.11

Table 7. Femur Rotation (No Pretensioning)

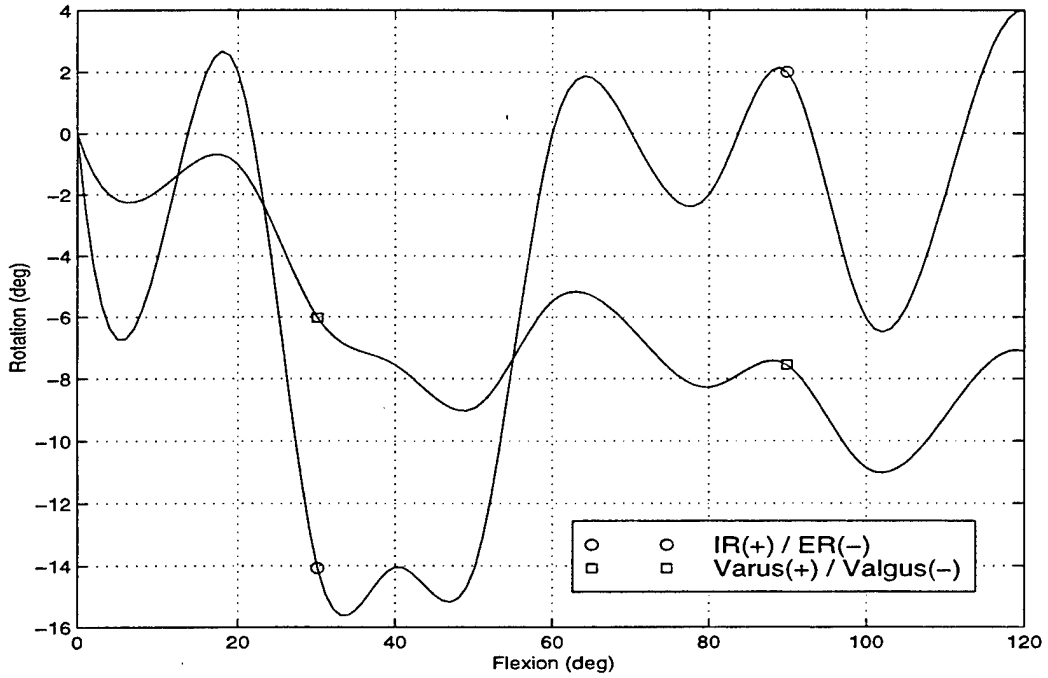

Figure 60. Femur Rotation (No Pretensioning)

c. Simulation Results (With Pretensioning)

Table 8 depicts the internal-external and varus-valgus rotations of the femur with Crowninshield pretensioning of ligaments. Figure 61 shows this graphically. The simulation showed a valgus orientation throughout flexion; this again is different than the Essinger's and Kurosawa's results.

FLEXION	INTERNAL(+)-EXTERNAL(-) (deg)	VARUS(+)-VALGUS(-) (deg)
10°	-8.00	-2.36
20°	-8.00	-3.34
30°	-12.05	-5.27
40°	-3.99	-4.97
50°	-3.99	-6.08
60°	-5.99	-8.30
70°	0	-6.37
80°	-2.01	-8.28
90°	2.00	-7.55
100°	2.01	-8.91
110°	9.88	-6.18
120°	9.95	-5.97

Table 8. Femur Rotation (Pretensioning)

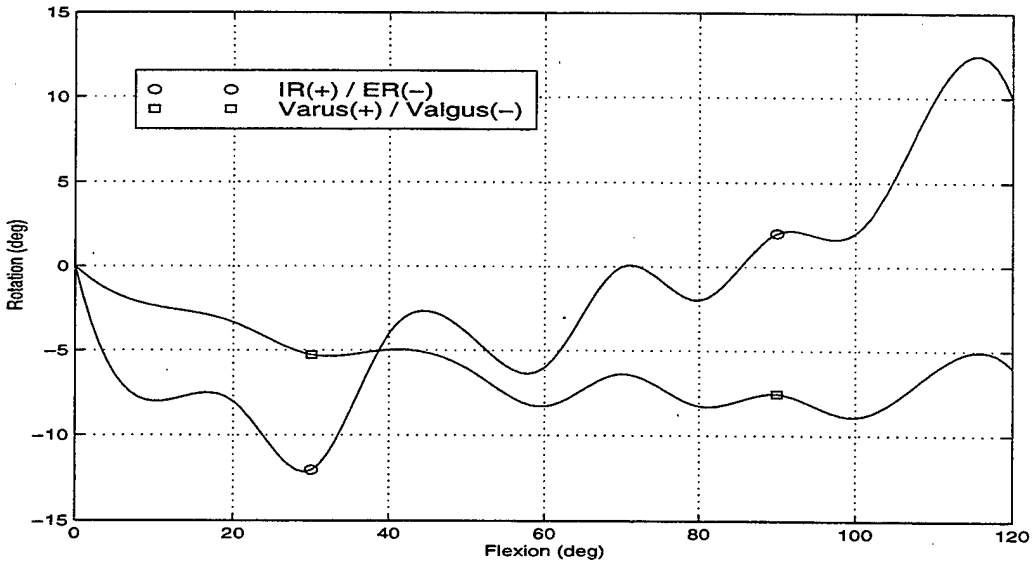

Figure 61. Femur Rotation (Pretensioning)

d. Simulation Results for ACL Deficient Knee

Table 9 depicts the internal-external and varus valgus rotations of the femur for an ACL deficient, Crowninshield pretensioned joint. Figure 61 shows this graphically. Because the ACL acts as a secondary restraint to internal rotation of the tibia [Ref. 4:p. 154], there should be increased external rotation of the femur. This was shown at 40°, 50° and 70° but there was a decrease in external rotation at 10°, 30°, 60°, 100° and 110°.

FLEXION	INTERNAL(+)-EXTERNAL(-) (deg)	VARUS(+)-VALGUS(-) (deg)
10°	-6.00	-1.57
20°	-8.00	-2.99
30°	-8.02	-4.58
40°	-7.99	-5.64
50°	-6.00	-7.04
60°	-3.99	-7.47
70°	-2.01	-7.56
80°	-2.01	-7.80
90°	2.00	-7.08
100°	3.99	-6.95
110°	5.93	-6.68
120°	9.95	-5.68

Table 9. Femur Rotation (ACL Deficient Knee)

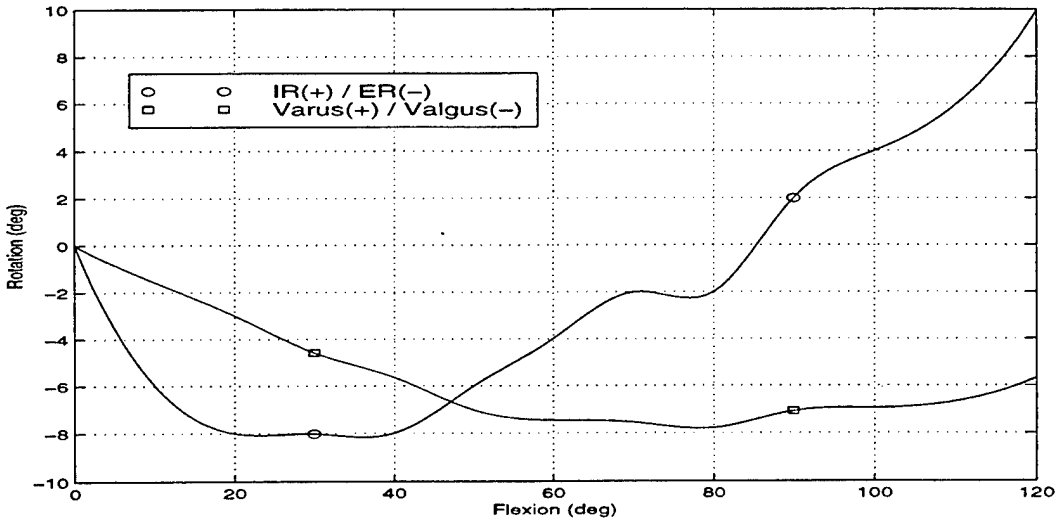

Figure 62. Femur Rotation (ACL Deficient Knee)

e. Simulation Results for PCL Deficient Knee

Table 10 depicts the internal-external and varus valgus rotations for a PCL deficient femur with Crowninshield pretensioning of ligaments. Figure 63 shows this graphically. The PCL acts as a major secondary restraint to external tibial rotation [Ref. 4p: 155]; therefore, in a PCL deficient knee, there should be an increase in internal rotation of the femur. The simulation did not show this.

FLEXION	INTERNAL(+)-EXTERNAL(-) (deg)	VARUS(+)-VALGUS(-) (deg)
10°	-8.01	-2.36
20°	-8.01	-3.34
30°	-12.05	-5.27
40°	-3.99	-4.97
50°	-3.99	-6.08
60°	-5.99	-8.30
70°	-12.10	-9.27
80°	-2.01	-8.28
90°	2.00	-7.55
100°	-6.06	-10.87
110°	-10.02	-11.77
120°	-8.04	-10.15

Table 10. Femur Rotation (PCL Deficient Knee)

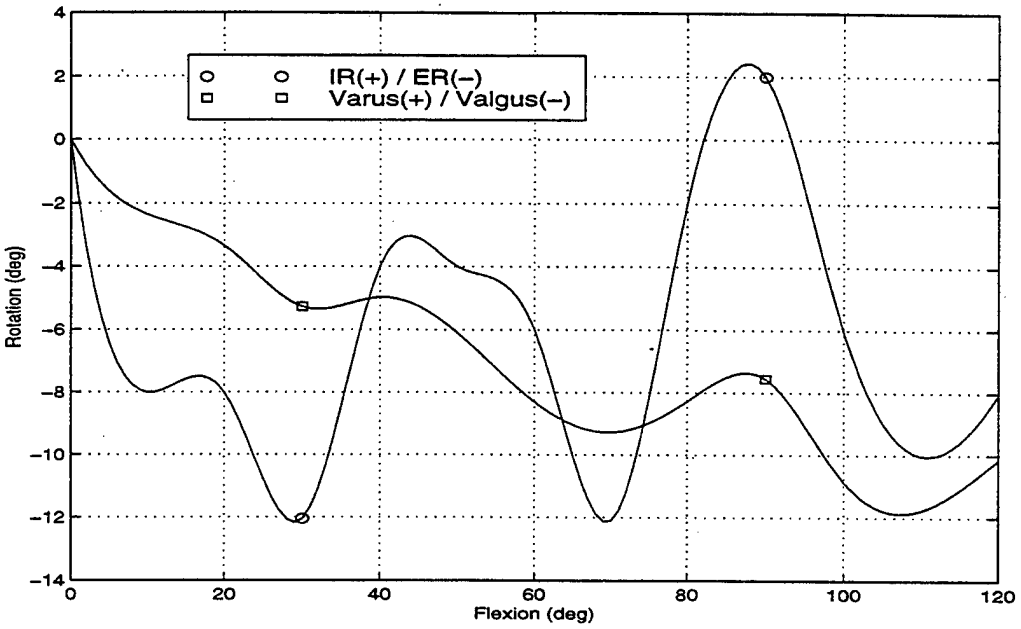

Figure 63. Femur Rotation (PCL Deficient Knee)

C. LIGAMENT LENGTH

Crowninshield, Essinger and Wang all computed the ratio of the length of the ligaments as the knee joint underwent flexion. Crowninshield and Essinger's ratios are presented graphically in Figures 64 and 65, respectively. Comparative graphs for the cases of no pretensioning, pretensioning, ACL deficient and PCL deficient knees are shown in Figures 66 through 69, respectively.

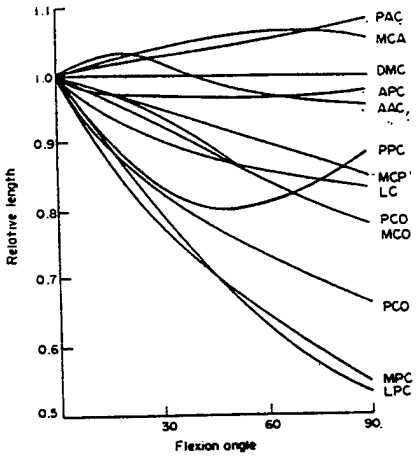

Figure 64. Crowninshield Ligament Length Graph from Ref. [1]

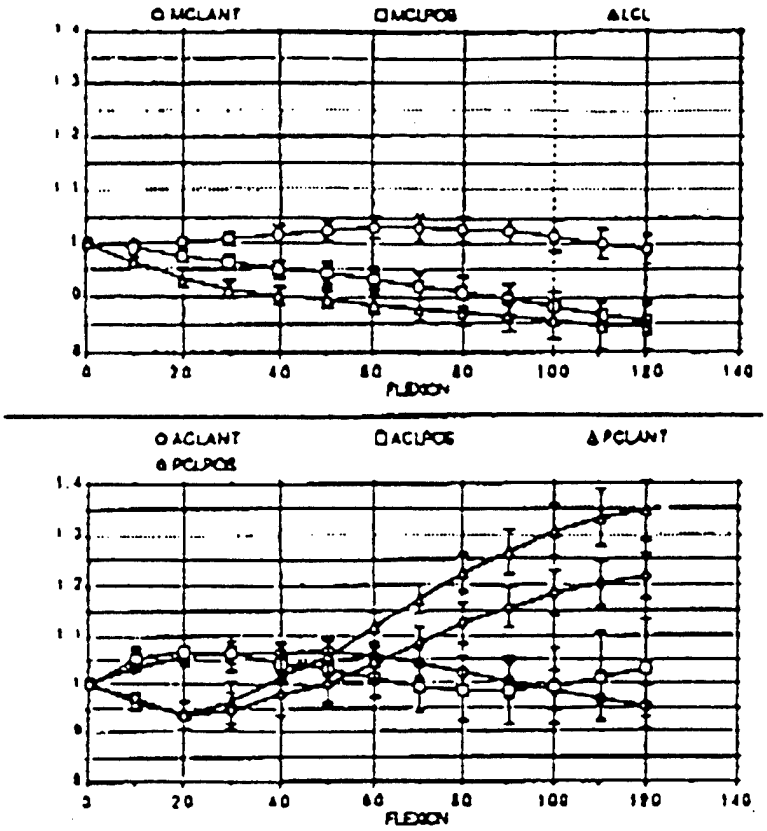

Figure 65. Essinger Ligament Length Graph from Ref. [2]

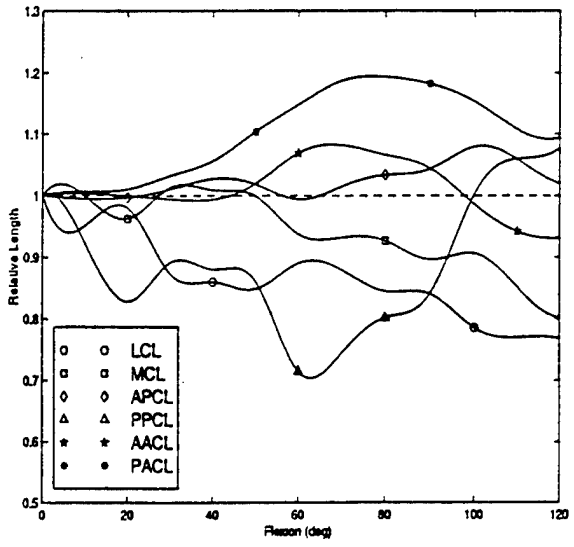

Figure 66. Ligament Length Graph

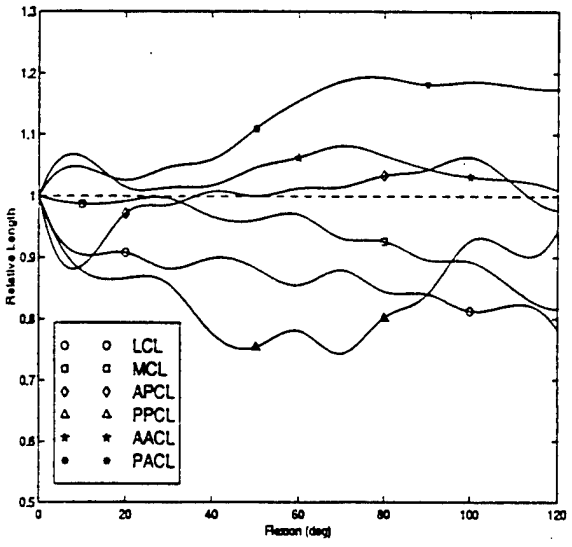

Figure 67. Ligament Length Graph (Pretensioning)

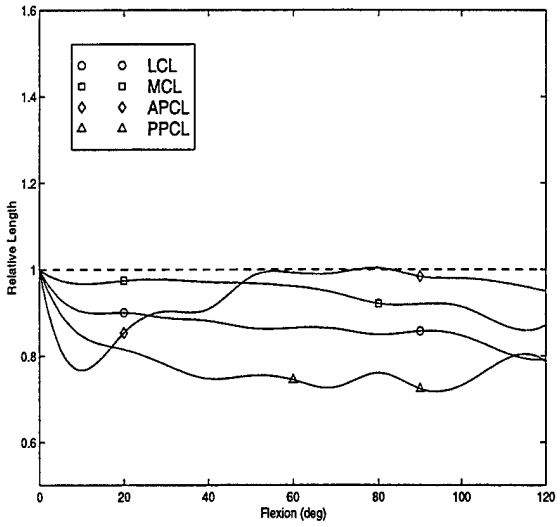

Figure 68. Ligament Length Graph (ACL Deficient Knee)

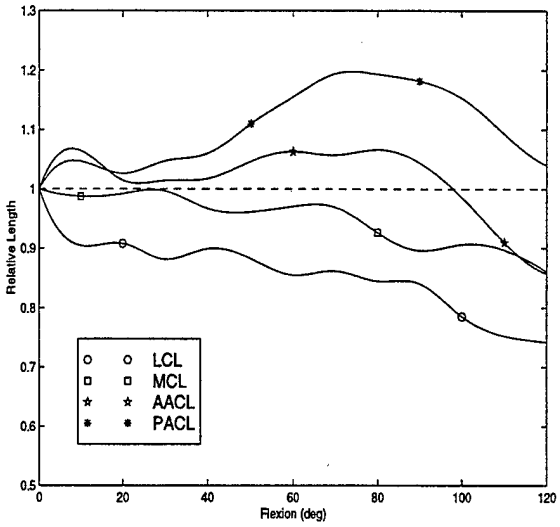

Figure 69. Ligament Length Graph (PCL Deficient Knee)

1. Anterior Cruciate Ligament

a. Previous Research

In his study, Crowninshield reported that Edwards (1970) found that the anterior cruciate was shortest at 60° of flexion [Ref. 1:p. 397]; Wang, however, found that the anterior cruciate lengthened throughout flexion [Ref. 9:p.590].

Girgis (1975) found that the function of each of the cruciate ligament could best be represented by separate anteromedial and posterolateral fibers and that these two fibers functioned in opposition [Ref. 1:p. 397]. According to Smillie, the anteromedial was taut in extension [Ref. 5:p. 205]. Crowninshield reported that the anterior fibers of the ACL reached a maximum at 15° of flexion [Ref. 1:p. 404]. Essinger found that the maximum length of the anterior ACL fibers occurred even later, at 45° flexion [Ref. 2:p. 1236].

Crowninshield reported that the posterior fibers of the ACL were longest in flexion [Ref. 1:p. 404]. Essinger's results were somewhat more specific: they showed that the posterior ACL fibers reached their maximum at 20° of flexion, decreased through 80° and increased again as flexion proceeded through 120° [Ref. 2:p. 1236].]. Smillie found the posterolateral fiber tightest in flexion [Ref. 5:p. 205]. Burks again found the converse to be true, i.e., in extension, the posterolateral fiber was tighter [Ref. 4:p. 75].

b. Simulation Results

In Table 11, the length ratios of the anterior and posterior fibers of the anterior cruciate ligament are provided for the cases of no pretensioning, Crowninshield pretensioning and PCL deficient cases for flexion along the path of the minimum potential energy. All ligaments are rationalized to their length at full extension.

Without pretensioning, the maximum length of the anterior fiber of the ACL was reached at 65°. With pretensioning, the length underwent a local maximum at 10° before decreasing and then increasing to its maximum length at 75°. This is not reflective of either Crowninshield or Essinger's results.

The posterior fiber of the ACL increases in length, reaching a maximum at approximately 73° in a knee without pretensioning. In a pretensioned knee the same general shape is reflected, however the posterior fiber is more taut after 90°. While these results agree with Smillie's observations, they do not agree with Crowninshield or Essinger. In a PCL deficient knee, the posterior ACL fiber qualitatively followed the results of the pretensioned knee; however, there appeared to be a greater shortening of the fiber after flexion through 78°.

FLEXION	NO PRETENSIONING		PRETENSIONING		PCL DEFICIENT KNEE	
	Ant ACL	Post ACL	Ant ACL	Post ACL	Ant ACL	Post ACL
10°	1.0039	1.0069	1.0641	1.0465	1.0641	1.0465
20°	.9996	1.0102	1.0145	1.0257	1.0145	1.0258
30°	.9942	1.0322	1.0139	1.0467	1.0139	1.0467
40°	.9938	1.0560	1.0172	1.0595	1.0172	1.0595
50°	1.0190	1.1030	1.0462	1.1094	1.0463	1.1094
60°	1.0689	1.1475	1.0626	1.1547	1.0626	1.1547
70°	1.0815	1.1869	1.0812	1.1869	1.0567	1.1939
80°	1.0658	1.1933	1.0658	1.1933	1.0658	1.1933
90°	1.0442	1.1817	1.0442	1.1817	1.0442	1.1817
100°	.9860	1.1528	1.0311	1.1863	.9860	1.1528
110°	.9419	1.1076	1.0256	1.1795	.9101	1.0927
120°	.9314	1.0940	1.0092	1.1737	.8578	1.0399

Table 11. Anterior Cruciate Ligament Fiber Length Ratios during Flexion

2. Posterior Cruciate Ligament

a. Previous Research

Edwards (1970) concluded that the PCL reached its longest length at full flexion [Ref. 9:p. 588]; however, Crowninshield reports that Wang's work in 1973 showed that the PCL reached its longest length at full extension [Ref. 1:p. 397]. Similar to the anterior cruciate, a more accurate representation of the function of the PCL can be realized by addressing the ligament as two separate bands: an anterolateral and a posteromedial fiber.

Hughston, according to Burks, found that the anterior fibers of the PCL are relaxed, therefore shortest, in extension and then lengthen in flexion [Ref. 4:p. 75]. Essinger reached a similar conclusion, reporting that the anterior PCL fibers were tight after 60°, thus implying that they were longer after 60° of flexion than before [Ref. 2:p. 1236]. However, Crowninshield concluded that the anterior PCL fibers had virtually no length change over the range of flexion [Ref. 1:p. 400].

For the posterior fibers of the PCL, both Hughston [Ref. 4:p. 75] and Crowninshield found that these were longest in extension [Ref. 1:p 400]. In contrast, Essinger found the opposite; the posterior fibers under taut after 40° of flexion, implying therefore lengthening after 40° [Ref. 2:p. 1236].

b. Simulation Results

In Table 12, the length ratios of the anterior and posterior fibers of the posterior cruciate ligament are provided for the thesis cases of no pretensioning, Crowninshield pretensioning, and ACL deficient cases of minimum potential energy. All ligaments are rationalized to their length at full extension. Without pretensioning, the anterior fiber of the PCL lengthened throughout most of flexion, reaching a maximum at 100°. In the pretensioned knee, the anterior fiber of the PCL initially decreased in length, reaching a minimum at just under 10° of flexion after which it steadily lengthened until just after 110°, when it again contracted. Neither of these results is in specific agreement with previous research, although the curve qualitatively resembles Essinger's graph. In the ACL deficient knee, the anterior fiber of the PCL showed greater contraction at 10°, virtually no change in length from 50° to 90°, after which it contracted.

The posterior fiber of the PCL was a maximum at full flexion in the non-pretensioned knee, reaching a minimum at 60° of flexion. In the pretensioned knee, the posterior fiber of the PCL showed opposite results: it was at a maximum at full extension. It reached its minimum length at approximately 70°. Similar results were reached for the lengthening of the posterior PCL fiber in an ACL deficient knee. The shape of the curve of the posterior fiber of the PCL also seems to qualitatively reflect Essinger's and Crowninshield's results.

FLEXION	NO PRETENSIONING		PRETENSIONING		ACL DEFICIENT KNEE	
	Ant PCL	Post PCL	Ant PCL	Post PCL	Ant PCL	Post PCL
10°	.9950	.9260	.8862	.8782	.7674	.8477
20°	.9970	.8277	.9718	.8663	.8540	.8154
30°	1.0104	.8912	.9852	.8575	.9038	.7794
40°	1.0271	.8801	1.0073	.7769	.9090	.7474
50°	1.0181	.8616	.9999	.7543	.9833	.7543
60°	.9937	.7147	1.0126	.7808	.9928	.7443
70°	1.0145	.7436	1.0145	.7436	.9923	.7276
80°	1.0334	.8022	1.0334	.8022	1.0039	.7609
90°	1.0428	.8399	1.0428	.8399	.9843	.7238
100°	1.0791	1.0027	1.0630	.9273	.9802	.7315
110°	1.0590	1.0600	1.0196	.9091	.9698	.7899
120°	1.0193	1.0773	.9772	.9441	.9507	.7872

Table 12. Posterior Cruciate Ligament Fiber Length Ratios during Flexion

3. Collateral Ligaments

There is excellent correlation in the shape of the lateral collateral and medial collateral ligament curves in the pretensioned case with the results of both Essinger and Crowninshield.

IV. CONCLUSIONS

It is difficult to make absolute comparisons with the results obtained by other researchers for several reasons. First, there are significant differences in the kinematic definitions utilized among researchers, particularly in the definition of rotation angles. Second, the lack of a universal coordinate system permits researchers to use any reference frame that is convenient for their work. Because of this, reference frames differ significantly between studies. Furthermore, they are not always adequately presented in the research, complicating the analysis process. Third, there is great individuality in the human anatomy. To account for statistical variability and to reach sound conclusions, large quantities of knees would have to be tested. The small numbers of knees examined in most studies does not render absolute the results achieved. This is amply demonstated in the differences shown between the work of various researchers.

Although in the previous chapter differences and similarities with previous research has been pointed out, the aforementioned factors preclude a direct, quantitative comparison. Qualitative comparisons, however, can be made. Incorporation of the pretensioning which is present at the position of full extension seems to be render more realistic results. Additionally, examination of the translation graph in the ACL deficient model shows that the ACL constrains the anterior motion of the tibia and plays a large role in early flexion. The translation graph from the PCL deficient model shows that the PCL constrains the posterior motion of the tibia and plays a larger role in the latter stages of flexion. The model is simplistic, but qualitatively, the results mimic real life.

There are several areas in which improvements can be made to this model. First, the ligaments and articular surfaces develop and work as a system. Since the topography

of the femur and tibia used in this study came from a foam-molded model, and the position of ligament attachment sites came from another study, these individual parts used did not comprise a system unto themselves. Thus, it is unknown if, in response to the ligament attachment sites utilized, the articular surfaces would have developed as molded.

Second, the reality of the three dimensional nature of the ligaments was not fully simulated. The ligaments were not evaluated to ensure that they had not passed through each other in moving to new orientations. Had this factor been examined, the permissible range of motion may have changed and thus altered the results.

Finally, the patella was not modeled in this simulation. As it provides another constraint to motion, it should have been included.

It is recommended that future research utilize cadaver knees. Furthermore, it is recommended that the full effect of the three dimensional reality of the ligaments is accounted for in order to ascertain the validity of the hypothesis and that the patella is incorporated in the model.

GLOSSARY OF MEDICAL TERMS

ANTERIOR – Directed toward the front.

ANTERIOR CRUCIATE LIGAMENT (ACL) – One of two ligaments which cross between the condyles of the femur holding the tibia and the femur together. The ACL is directed from posteriolateral on the femur to anteriomedial on the tibia.

CONDYLE – A rounded projection at the end of a bone that articulates with another bone.

DISTAL – Farthest point from a line of reference, typically the body center.

EPICONDYLE – Bony prominence found on either side of the femur corresponding to the femoral origin of the medial and lateral collateral ligaments.

FEMUR – The thigh bone which extends from the hip to the knee.

LATERAL – Situated to the side or directed to the side.

LATERAL COLLATERAL LIGAMENT – The major ligament attaching the femur to the tibia on the lateral side of the knee.

LIGAMENT – A strong fibrous band of connecting tissue which binds the articular ends of bones to limit motion or to hold body organs in place.

MEDIAL – Situated to the middle or directed to the middle.

MEDIAL COLLATERAL LIGAMENT – The major ligament attaching the femur to the tibia on the medial side of the knee.

POSTERIOR – Directed toward the rear.

POSTERIOR CRUCIATE LIGAMENT (PCL) – One of two ligaments which cross between the condyles of the femur holding the tibia and the femur together. The PCL is directed from anterioedial on the femur to posteriolateral on the tibia.

PROXIMAL – Closest point from a line of reference, typically the body center.

TIBIA – The shin bone which extends from the knee to the ankle.

VALGUS – The femur is bent outward with respect to the tibia. Knock kneed.

VARUS – The femur is bent inward with respect to the tibia. Bowlegged.

Definitions derived from *The New Webster's Medical Dictionary*, *The Knee: Form, Function, and Ligament Reconstruction* by W. Muller, *and Knee Ligaments: Structure, Function, Injury, and Repair* ed. D. Daniel, W. Akeson, and J. O'Connor

LIST OF REFERENCES

1. Crowninshield, R., Pope, M.H. and Johnson, R.H., "An Analytical Model Of The Knee," *Journal of Biomechanics* , vol. 9, no. 6, pp. 397-405, Great Britain, 1976

2. Essinger, J. R., Leyvraz, P. F., Heegard, J. H., Robertson, D. D., " A Mathematical Model for the Evaluation of the Behaviour During Flexion of Condylar-type Knee Prostheses," *Journal of Biomechanics*, vol. 22, no. 11/12, pp. 1229-1241, Great Britain, 1989

3. Wismans J.,Veldpaus F., Janssen, J. Huson , Struben P., "A Three-Dimensional Mathematical Model Of The Knee-Joint," *Journal of Biomechanics*, vol. 13, no. 8, pp. 677-685, Great Britain, 1980

4. Daniel, D., Akeson, W., O'Connor, J., *Knee Ligaments - Structure, Function, Injury, and Repair*, Raven Press, 1990

5. Muller, W., *The Knee - Form, Function, and Ligament Reconstruction*, Springer-Verlag, 1983

6. Webpage: http://web1.whs.osd.mil. under Personnel, Military Personnel

7. Private conversation with DeMaio, M., Department of Orthopaedic Surgery, National Naval Medical Hospital, Bethesda, MD, 1998

8. Blankevoort L., R. Huiskes and A. de Lange, "The Envelope Of Passive Knee Joint Motion," *Journal of Biomechanics*, vol. 21, no. 9, pp. 705-720, Great Britain, 1988

9. Wang, C.J., Walker, P.S., "The Effects of Flexion and Rotation on the Length Patterns of the Ligaments of the Knee," *Journal of Biomechanics*, vol. 6, no. 7, pp. 587-596, Great Britain, 1973

10. Kurosawa, H., Walker, P.S., Abe, S., Garg, A., Hunter, T., "Geometry And Motion Of The Knee For Implant And Orthotic Design," *Journal of Biomechanics*, vol. 18, no. 7, pp. 487-499, Great Britain, 1985

BIBLIOGRAPHY

Blacharski, P.A., Somerset, J.H., Murray, D.G., "A Three-Dimensional Study of the Kinematics of the Human Knee," *Journal of Biomechanics*, vol. 8, no. 6, pp. 375-384, Great Britain, 1975

Blankevoort L., R. Huiskes and A. de Lange, "Helical Axes of Passive Knee Joint Motions," *Journal of Biomechanics*, vol. 23, no. 12, pp. 1219-1229, Great Britain, 1990

DeMaio, M., Adkison, D., Kwon, Y.W., "Continuous Motion Kinematics of the Loaded Human Cadaveric Knee: A Comparison between the Posterior Cruciate Intact, Deficient and Reconstructed States," (to be submitted for publishment at a future date)

Hollister, A.M., Jatana, S., Singh, A., Sullivan, W.W., Lupichuk, A.G., "The Axes of Rotation of the Knee", Clinical Orthopaedics and Related Research, no. 290, pp.259-267, Philadelphia, PA, 1993

Seering, W.P., Piziali, R.L., Nagel, D.A., Schurman, D.J., "The Function of the Primary Ligaments of the Knee in Vaurs-Valgus and Axial Rotation," *Journal of Biomechanics*, vol. 13, no. 9, pp. 785-794, Great Britain, 1980

Trent, P.S., Walker, P.S., Wolf, B., "Ligament Length Patterns, Strength and Rotational Axes of the Knee Joint," *Clinical Orthopaedics and Related Research*, no.117, pp. 263-270, Philadelphia, PA, 1976

INITIAL DISTRIBUTION LIST

1. Defense Technical Information Center 2
   8725 John J. Kingman Rd., STE 0944
   Ft. Belvoir, Virginia 22060-6218

2. Dudley Knox Library 2
   Naval Postgraduate School
   411 Dyer Rd.
   Monterey, California 93943-5101

3. Director, Education and Training 1
   MCCDC, Code C46
   1019 Elliot Rd.
   Quantico, Virginia 22134-5027

4. Director, Marine Corps Research Center 2
   MCCDC, Code C40RC
   2040 Broadway Street
   Quantico, Virginia 22134-5107

5. Director, Studies and Analysis Division 1
   CMCDC, Code C45
   300 Russell Road
   Quantico, Virginia 22134-5130

6. Marine Corps Representative 1
   Naval Postgraduate School
   Code 037, Bldg. 234, HA-220
   699 Dyer Road
   Monterey, California 93940

7. Marine Corps Tactical Systems Support Activity 1
   Technical Advisory Branch
   Attn; Maj J.C. Cummiskey
   Box 555171
   Camp Pendleton, California 92055-5080

8. Department Chairman, Code PH 1
   Department of Physics
   Naval Postgraduate School
   Monterey, California 93943-5000

9. Professor Young W. Kwon, Code ME/KW 1
Department of Mechanical Engineering
Naval Postgraduate School
Monterey, California 93943-5002

10. Professor William B. Maier, Code PH/WB 1
Department of Physics
Naval Postgraduate School
Monterey, California 93943-5000

11. LtCol Patricia F.Warren 3
1417 Southwestern Road
Grove City, Ohio 43123